Friedrich-Alexander-Universität Erlangen-Nürnberg

Institute for Electronics Engineering

Prof. Dr.-Ing. Dr.-Ing. habil. Robert Weigel

Prof. Dr.-Ing. Georg Fischer

Master Thesis

Course of Study

Industrial Engineering

by

Carlos Martínez Cantón

on the Subject

Optimization of the transmitter setup for a molecular communication link based on superparamagnetic iron nanoparticles

Supervisors: Prof. Dr.-Ing. Georg Fischer

Dr. rer. nat. Jens Kirchner

Begin: 15.04.2018

Submission: 15.10.2018

Optimization of the transmitter setup for a molecular communication link based on superparamagnetic iron nanoparticles

Erklärung

Ich versichere, dass ich die Arbeit ohne fremde Hilfe und ohne Benutzung anderer als der gegebenen Quellen angefertigt habe und dass die Arbeit in gleicher oder ähnlicher Form noch keiner anderen Prüfungsbehörde vorgelegen hat und von dieser als Teil einer Prüfungsleistung angenommen wurde.

Alle Ausführungen, die wörtlich oder sinngemäβ übernommen wurden, sind als solche gekennzeichnet.

Erlangen, den 15. Oktober 2018

Carlos Martínez Cantón

Kurzfassung

Die Suche nach innovativen Anwendungen in den Bereichen Biomedizin und Nanotechnologie kommt dem weiteren Fortschritt in der molekularen Kommunikationsforschung zugute. Dennoch ist ein voll funktionsfähiges künstliches molekulares System noch keine Realität. Das Institut für Elektronik der FAU hat ein experimentelles molekularkommunikatives Testbed auf Basis magnetischer Nanopartikel entwickelt, das sich als effektiv bei der Übertragung von Bitsequenzen erwiesen hat, die von SPIONs kodiert werden. Im Rahmen dieser Arbeit wurde eine Optimierung des Senders dieses Setups implementiert und getestet. Diese Optimierung basiert auf der Lenkung von SPIONs über einen gewünschten Weg nach einer Aufspaltung unter Verwendung der magnetischen Kraft, die von einem Elektromagneten erzeugt wird, der sich taktisch in der Nähe der Röhren befindet, in denen die Nanopartikel fließen. Die Größe des Elektromagneten wurde im Verhältnis zu der Röhrengröße des Systems ausgewählt. Außerdem wurde eine elektronische Steuerschaltung zum automatschen Schalten des Elektromagneten entworfen und auf einem Protoboard montiert. Die Messung der Mengen an magnetischen Partikeln in den Röhren des Systems erfolgt unter Verwendung einer Suszeptometerspule, einer elektronischen Vorrichtung, durch die sich die magnetischen Partikel bewegen und ein elektronisches Signal erzeugen.

Es werden experimentelle Ergebnisse für magnetische Suszeptibilitätsänderungen in beiden Kanälen nach dem Y-Verbinder vorgestellt. Sie fielen nicht wie erwartet aus, weshalb Empfehlungen gegeben werden, um zuverlässige Messungen zu erhalten und die vorgestellte Forschungsarbeit weiter voranzutreiben.

Abstract

The search for innovative applications in the fields of biomedicine and nanotechnology benefit the further advance in molecular communication research. Nevertheless, a fully-functional artificial molecular system is not yet a reality. Institute for Electronics Engineering from FAU has developed an experimental molecular communication testbed based on magnetic nanoparticles, which has demonstrated to be effective in the transmission of bit sequences encoded by SPIONs. As part of this work, an optimization of the transmitter of this setup is implemented and tested. This optimization is based on the steering of SPIONs through a desired path after a splitting by use of the magnetic force generated by an electromagnet, which is located tactically in the proximity of the tubes where the nanoparticles flow. The electromagnet size has been selected in proportion to the tubes size of the system. Also, an electronic control circuit to switch automatically the electromagnet has been designed and mounted on a protoboard. Measuring of magnetic particles amount in the tubes of the system is accomplished using a susceptometer coil, an electronic device where the magnetic particles move through and generate an electrical signal.

Experimental results for magnetic susceptibility changes in both channels after the Y-connector are presented. They have not been as expected, thus, recommendations in order to acquire more reliable measurements and further advancing in the presented research work are given.

Abbreviations

FAU	Friedrich-Alexander-Universität Erlangen-Nürnberg
SPION	Superparamagnetic Iron Oxide Nanoparticle
MC	Molecular Communication
TX	Transmitter
RX	Receiver
pH	Potential of Hydrogen
MRI	Magnetic Resonance Imaging
GUI	Graphical User Interface
DC	Direct Current
BJT	Bipolar Junction Transistor
LED	Light Emitting Diode
PIC	Programmable Intelligent Computer

Contents

Chapter 1

Introduction

The interest in molecular communication is growing due to the need of transmitting information at micro- or nanoscale. Communication using small particles in areas impenetrable for electromagnetic waves is an alternative for many applications in the field of biomedicine or nanotechnology, such as drug targeting or monitoring of chemical reactors [1]. Nevertheless, a fully-functional artificial communication system has not been realized yet.

Institute for Electronics Engineering from Friedrich-Alexander-Universität Erlangen-Nürnberg (FAU) has developed an artificial molecular communication system in the size range of several cm [2], but now realizing it at nanoscale remains a challenge. The testbed emulates blood vessels by use of tubes, where superparamagnetic iron oxide nanoparticles (SPIONs) are transported and used as information carriers. These particles are a type of artificial particles well-established in biotechnology and biocompatible [3]; they are also clinically safe and do not interfere with other chemical processes like acids and bases would do, which makes them attractive for applications such as the monitoring of chemical reactors where particles stored in a reservoir could be released upon an event like the detection of a defect. Moreover, they can be attracted by an external magnetic field generated by a magnet or a solenoid and externally visualized, which can help detection and supervision.

The mentioned setup above is based on the injection and transportation of these magnetic nanoparticles along a propagation tube using two electronic pumps. The particles are transported a certain distance until being detected by an electric coil, whose current is affected by the magnetic nanoparticles moving through its core. The signal detected by the coil is used to determine the transmitted binary sequence. When particles move

through the coil, binary “1”is detected; if particles are absent, this is interpreted as binary “0”.

The system works properly and it is capable of transmitting encoded messages as binary bits. Now, the goal is to optimize the transmission setup trying to guide the particles through a specific path. In this work, one alternative is proposed, which consists in steering the magnetic nanoparticles with a controlled external magnetic field generated by an electromagnet. It is located tactically in the proximity of the propagation tube so that the nanoparticles flow towards the desired direction after a Y-connector.

In the following chapter, basics of molecular communication, magnetism, SPIONs and electromagnets are given. Chapter 3 summarizes briefly the current testbed developed by Institute for Electronics Engineering from FAU. Chapter 4 presents the new setup it has been tested together with the electronic circuit designed to control automatically the switch of the electromagnet. In Chapter 5 the results acquired from several experiments with the new testbed are presented. The present work concludes by a summary of results and an outlook for future improvements is suggested.

Chapter 2

Fundamentals

This chapter presents some fundamentals of molecular communication, magnetism, magnetic nanoparticles that are used in molecular communication systems, electromagnets and its magnetic theory. These fundamentals shall help to understand the basic molecular communication notions and the basic physics and electromagnetism concepts in the field of electromagnets.

2.1 Molecular Communication

Modern communication systems work with electrical or electromagnetic signals. However, there are applications in which this is inefficient or inappropriate, like for instance, at sizes extremely small. This is the case of communication among devices at micro- or nanoscale (e.g., nanorobots), due to restrictions regarding the antenna size and the wavelength of the electromagnetic signal [4]. Because of these limitations, appears the necessity to search for innovative communication systems that use other sort of propagation signal.

At the same time, progresses in nanotechnology, which make possible to miniaturize a lot of devices, and the development in biotechnology, boost the scale reduction of information systems. From here emerges the idea of molecular systems at sizes of micro- or nanometers that are inspired by nature. Molecular communication (MC) bases on a biological form of communication, where chemical signals are used to transfer information, likewise many living beings do it through molecules.

As illustrated in Figure 2.1, a MC system is composed of three main components, like conventional communication systems: a transmitter (TX), a receiver (RX) and a channel. In MC, the information is contained in particles whose size is micrometric or nanometric. These particles can be biological (like hormones, proteins, pheromones, etc.) or synthetic (like SPIONs). The TX provides the energy required to generate and propagate the particles through the channel, which tend to be an aqueous one (like blood in living organisms) or a gaseous one (like air). When a particle acting as information carrier arrives at the RX, then it is detected and decoded in order to interpret the information included in the particle.

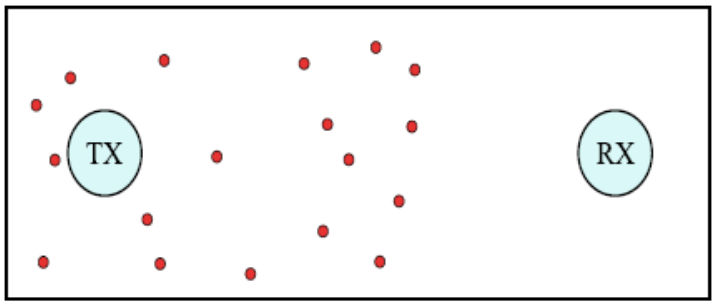

Figure 2.1: Schematic representation of molecular communication between a transmitter (TX) and a receiver (RX). Particles released by the TX are the information carriers and are represented as red circles [5].

The main advantages of MC compared to conventional communication systems are: the first one is that MC signals can be biocompatible, like SPIONs used for drug targeting applications (there are others that are not, like acids and bases, which interfere with other chemical processes) and, thus, with possibility to be used in living organisms. The second one is the greater energy efficiency of MC systems. Furthermore, it is suitable for use in nanomachines. Regarding its general disadvantages, molecules propagation presents randomness, which implies noise in the propagation signal. Also, the propagation time is rather long and the biological particles can be affected by their environment (temperature, pH, among others). Even so, MC signals are ideal for many applications where use of electromagnetic signals is not appropriate or not desirable.

There is a large number of possible applications for MC in different fields, some of which are:

- **Health sector**: targeted drug delivery, reconstruction of tissues and damaged organs, modification of the sequences of human genes, localization and reaction with malicious cells (i.e., cancer).
- **Environment**: environmental monitoring to detect polluting and toxins, control the quality of water and food.
- **Manufacturing**: develop new materials and manufacturing processes, quality control by identification of defects in products.
- **Others**: interact with insects, animals or plants, monitoring of infrastructures, robotic communication.

Although MC systems offer a new option of communication and have a high applicability in several fields, they still present limits. Thus, more experimentation is required in order to further advance molecular communication research.

In next section, basics of magnetism and an explanation of a type of synthetic magnetic particles used in molecular communication systems (SPIONs) are given.

2.2 Magnetism

Magnetism is the phenomenon by which materials attract or repel other materials from a distance. All substances have magnetic properties. It is well-known the magnetic properties of iron, which is used in compasses or components from electric systems. But, other materials different from iron have also magnetic properties, although to a lesser extent.

Magnetic fields are generated by the movement of an individual electric charge or a combination of electric charges (electrical current); they can also be produced by some materials like permanent magnets. When a charged particle spin (like electrons spin at atomic scale), it generates a magnetic dipole. Applying an external magnetic field on the material, their magnetic dipoles align to the field causing a magnetic moment in the material.

When an external magnetic field $\vec{H}$ (units A/m) reaches a material, the magnetic field $\vec{B}$ (units Tesla) induced in it is [6]:

$$\vec{B} = \mu_0(\vec{H} + \vec{M}) \tag{2.1}$$

where μ_0 is the permeability of vacuum (1.257×10^{-6} H/m) and $\vec{M}$ (units A/m) is the magnetization of the substance, which is produced due to the alignment of the magnetic dipoles of the substance with the external field.

The magnetic susceptibility χ (dimensionless in SI units) is a magnitude that relates this magnetization and the external magnetic field [6]:

$$\vec{M} = \chi\vec{H} \tag{2.2}$$

It is a characteristic magnitude of materials that indicates how sensitive the material is to a magnetic field. The greater it is, the more magnetizable the material is.

According to the response of a material in the presence of an external non-uniform magnetic field, it is classified as diamagnetic, paramagnetic or ferromagnetic. Some examples of diamagnetic materials are water, copper or lead; some of paramagnetic ones are aluminium or magnesium; some of ferromagnetic ones are iron, nickel or cobalt.

Diamagnetic substances ($\chi < 0$) are repelled from regions with high magnetic field, whereas paramagnetic ones ($\chi > 0$) are attracted to them. On the other hand, ferromagnetic materials ($\chi > 0$) present magnetic properties, even when the applied magnetic field is removed. The attraction of ferromagnetic substances towards high magnetic areas is stronger than that of paramagnets.

In this work, SPIONs are used as information carriers in the molecular communication testbed. In order to understand better their behaviour under the influence of an external magnetic field, some fundamentals of paramagnetism and superparamagnetism are presented in the following.

2.2.1 Paramagnetism

Paramagnetic materials are those that in the presence of a magnetic field gradient, move towards the area with higher magnetic field intensity. These substances experience the same type of attraction and repulsion like magnets. However, they are not permanently magnetized, since when the applied magnetic field disappears, also the induced magnetic alignment of their magnetic dipoles does (see Figure 2.2) and, thus, causing its demagnetization.

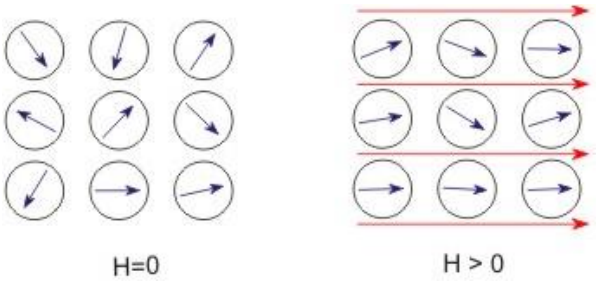

Figure 2.2: Schematic representation of magnetic dipoles of a paramagnetic material under the influence of an applied magnetic field gradient. The magnetic dipoles are randomly oriented in the absence of a magnetic field (the net magnetic moment of the material is zero). When a magnetic field gradient is applied, the magnetic dipoles align themselves in the same direction of the field [7].

The magnetic permeability of a substance (μ) is its capacity to attract or being passed through by a magnetic field; the relative magnetic permeability (μ_r) is its magnetic permeability compared to vacuum magnetic permeability (μ_0):

$$\mu_r = \frac{\mu}{\mu_0} \tag{2.3}$$

Paramagnetic materials are slightly more magnetically permeable than the vacuum ($\mu \geq 1$) and have a very small and positive magnetic susceptibility ($\chi > 0$). For that reason, they are weakly attracted by magnetic fields and as previously mentioned, they do not keep their properties as soon as the magnetic field disappears.

This weak attraction force is due to the fact that the magnetic dipoles of the material are completely disordered (see Figure 2.2) in such natural state, causing that the magnetic field was only able to orient them lightly.

The magnetization of a paramagnet is determined by Curie's law:

$$M = C \cdot \frac{B}{T} \tag{2.4}$$

where T is the absolute temperature in Kelvin and C a constant that depend on the material. From this law, we can observe that paramagnetic materials tend to be more magnetic as higher is the applied magnetic field, and less magnetic as higher is the temperature. Nevertheless, when the paramagnetic material is near its magnetic saturation *M*s (moment in which most of its magnetic dipoles are aligned to the field), then this law is not applicable, since as Figure 2.3 shows, the relation magnetization-magnetic field is not linear.

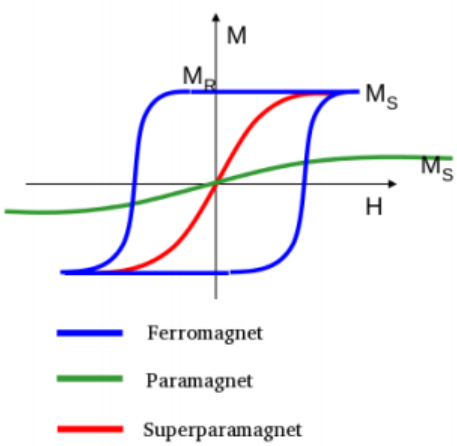

Figure 2.3: Magnetization curves for ferromagnetic, paramagnetic and superparamagnetic materials. *M*s: magnetic saturation; M_R: remnant magnetization [8].

Among paramagnetic materials exists special ones called superparamagnetics. In next section, a brief description of them is presented.

2.2.2 Superparamagnetism

Superparamagnetism is a phenomenon presented in some materials, which show paramagnetic properties under specific critic temperatures. It occurs at small scale, like in nanoparticles of approximately 20 nm or less, when the energy required to change the direction of the particles is similar to the ambient thermal energy. It causes that a significant number of particles of the material change direction randomly over short periods. In such state, they act as paramagnetic particles, allowing its magnetization under the influence of an applied magnetic field. However, they present a greater magnetic susceptibility than paramagnetic particles.

Superparamagnetic particles have a remnant magnetisation M_R (persistent magnetization on the material when the applied magnetic field is removed) of zero, which implies they can be demagnetized rapidly, even when they are saturated ($M = M$s). They are magnetized in the presence of a magnetic field, but they are demagnetized as soon as the field disappears. Consequently, their *M-H* curve shows no hysteresis (see Figure 2.3); this property is important for reducing the tendency of the particles to agglomerate [9].

These kind of substances are used for magnetic resonance imaging (MRI), for drug delivery, for cell separation and cell labelling applications, among others [10].

In the following, a type of superparamagnetic particles that are used in molecular communication systems is described.

2.2.3 Superparamagnetic Iron Oxide Nanoparticles

Superparamagnetic iron oxide nanoparticles (SPIONs) are a kind of particles with sizes around few tens of nm which are used in many research studies regarding biotechnology and biomedicine. Their widespread use is due to the large number of possible applications where they can be used, especially on health sector, as well as their low cost, strong adsorption capacity, easy separation and enhanced stability [11].

SPIONs are composed of maghemite, magnetite or hermatite [12] and they can be synthetized by physical, chemical or biological methods (e.g., co-precipitation, high temperature decomposition, etc.) [13].

They present superparamagnetic properties, thus, in a natural state their total net magnetic moment is zero (the magnetic dipoles of the nanoparticle are randomly oriented), but under the influence of an external magnetic field they are magnetized; they become again

demagnetized as soon as the magnetic field is removed. This performance makes these particles very useful for applications like targeted drug delivery, where a drug is loaded on the coating of the nanoparticle (see Figure 2.4) and next, it is guided and retained in the desired area of the body because of the effect of an external magnetic field generated by a magnet or electromagnet. This is similar to the posed goal of this thesis, with the difference that we only want to steer the SPIONs, not retain them in a specific area.

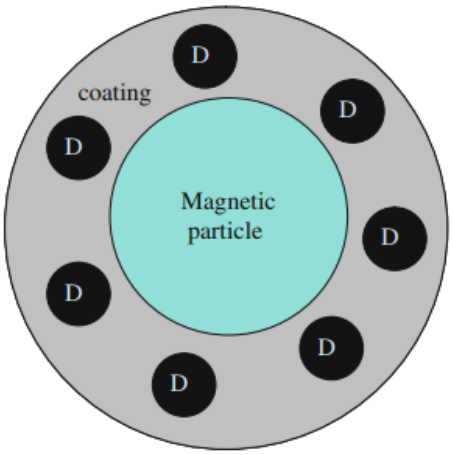

Figure 2.4: Magnetic particle with coating. D refers to functional groups [9].

SPIONs have many other biomedical applications such as contrast agents for diagnosis of cancer or cardiovascular diseases through MRI, for tracking cells migration, used in stem cells therapy, hyperthermia treatments, etc. [13].

In this thesis, we use an electromagnet in order to guide these particles through a specific path. Next, a brief explanation of these components is shown.

2.3 Solenoids and Electromagnets

In order to guide SPIONs through a desired way, an electromagnet is used. This component steers the nanoparticles under the influence of a magnetic field or more precisely, under the influence of a magnetic field gradient.

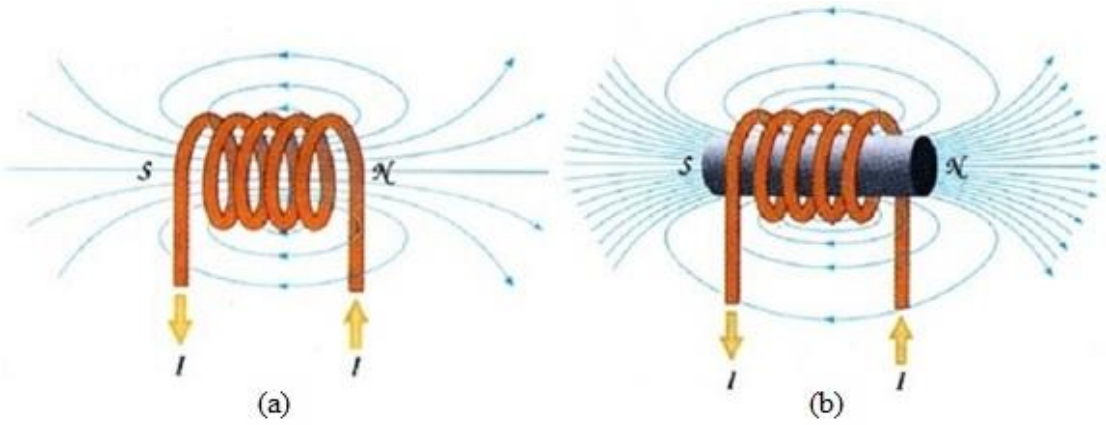

Figure 2.5: Magnetic field lines generated by solenoids (a) and electromagnets (b) [14].

As Figure 2.5 shows, a solenoid is a coil composed of a conductive wire with helicoidal shape that produces a magnetic field when an electric current is passed through it. It behaves as a magnet, with a north pole and a south pole; the magnetic field lines go from the north to the south pole outside and from south to north inside the coil. The magnitude of the generated magnetic field inside the solenoid is given by:

$$B = \frac{\mu_0 NI}{L} \tag{2.5}$$

where μ_0 is the magnetic permeability of the vacuum, N the number of turns, I the current (units A) and L (units m) the length of the solenoid.

If a ferromagnetic core is introduced inside the coil, then the component is called electromagnet. This core increases the magnitude of the magnetic flux density in the solenoid and raises the effective permeability of the magnetic path. Then the magnetic field inside the component is given by:

$$B = \frac{\mu NI}{L} \tag{2.6}$$

where μ (SI units, NA^{-2}) is the absolute magnetic permeability of the material of the core.

2.3.1 Magnetic Force Generated by an Electromagnet on a SPION

Since in this work and many other applications in biomedicine require to manipulate the path of the nanoparticles, it is appropriate to understand the force required to do so. Some research studies about this topic, where several magnets or magnetic elements of different geometries are taking into account, have been accomplished; see for example references [15], [16]. But not for the specific case of an electromagnet.

As indicated in reference [6], the general equation for the magnetic force generated by a non-homogenous magnetic field on a nanoparticle in solution is:

$$\vec{F}_m = \frac{\chi_p - \chi_s}{\mu_0} V(\vec{B} \cdot \vec{\nabla})\vec{B} \tag{2.7}$$

being χ_p and χ_s the magnetic susceptibilities of the particle and the solvent, respectively. In this work we use SPIONs dispersed in an aqueous suspension. In particular, lauric acid coated SPIONs ($SPION^{LA}$) with a hydrodynamic particle radius of 27.5 nm are used, thus, χ_p is the magnetic susceptibility of a SPION (7.28×10^{-3} in SI units) and χ_s is the magnetic susceptibility of the water (-9.04×10^{-6} in SI units) .

Consider now the case of this work, where the magnetic force generated by an electromagnet is used to divert the trajectory of SPIONs flowing in the system in order to steer them through the correct path after a splitting, as illustrated in Figure 2.6.

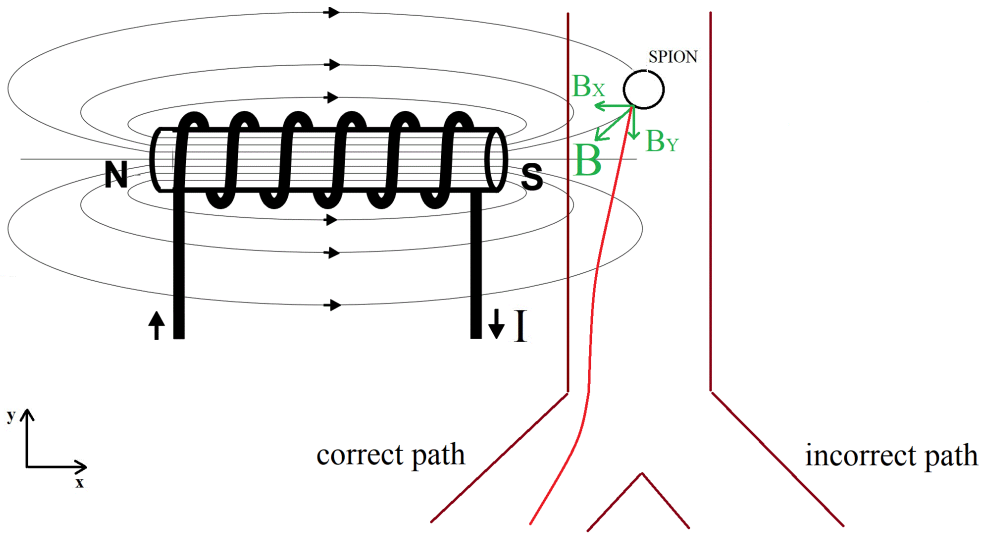

Figure 2.6: Schematic of the steering of a SPION through a specific path (described as correct path) by the influence of the magnetic field generated by an electromagnet. In red colour the expected SPION trajectory.

Assuming that a SPION is spherical with a radius *R*, its volume is $V = \frac{4\pi R^3}{3}$. Therefore, equation (2.7) transforms into:

$$\vec{F}_m = \frac{(\chi_p - \chi_w)}{\mu_0} \cdot \frac{4\pi R^3}{3} \cdot \begin{pmatrix} B_x \frac{\partial B_x}{\partial x} + B_y \frac{\partial B_x}{\partial y} + B_z \frac{\partial B_x}{\partial z} \\ B_x \frac{\partial B_y}{\partial x} + B_y \frac{\partial B_y}{\partial y} + B_z \frac{\partial B_y}{\partial z} \\ B_x \frac{\partial B_z}{\partial x} + B_y \frac{\partial B_z}{\partial y} + B_z \frac{\partial B_z}{\partial z} \end{pmatrix} \tag{2.8}$$

where χ_p is the magnetic susceptibility of the SPION and χ_w the magnetic susceptibility of the water. To find the magnetic force, thus, it is required to know the components of the magnetic field $\vec{B}$ vector as well as the various partial derivatives of the magnetic field.

The lack of information regarding the magnetic field generated in external points from an electromagnet, complicate the resolution of equation (2.8). For the present work, it has not been considered essential to find a specific solution, rather the current work consists in studying the possibility to guide the magnetic nanoparticles under the influence of a magnetic field, regardless of the value it has.

Chapter 3

Current Molecular Communication System

In this chapter a brief description of the operation of the current artificial molecular system developed by Institute for Electronics Engineering from FAU is presented. The testbed has been demonstrated to be effective sending information encoded as bits through SPIONs. Now, the main purpose of this work is to optimize the transmitter setup of this system, thus, a proper understanding of its working is required.

The system developed by FAU (see Figure 3.1) consists in a molecular communication system based on information transmission through encoded messages by SPIONs. Specifically, the testbed uses lauric acid coated SPIONs ($SPION^{LA}$) as information carriers because of their magnetic properties. To see detailed parameters of these nanoparticles, the diameter and length of the tubes, flow rates of the pumps, etc., see Table I from reference [2].

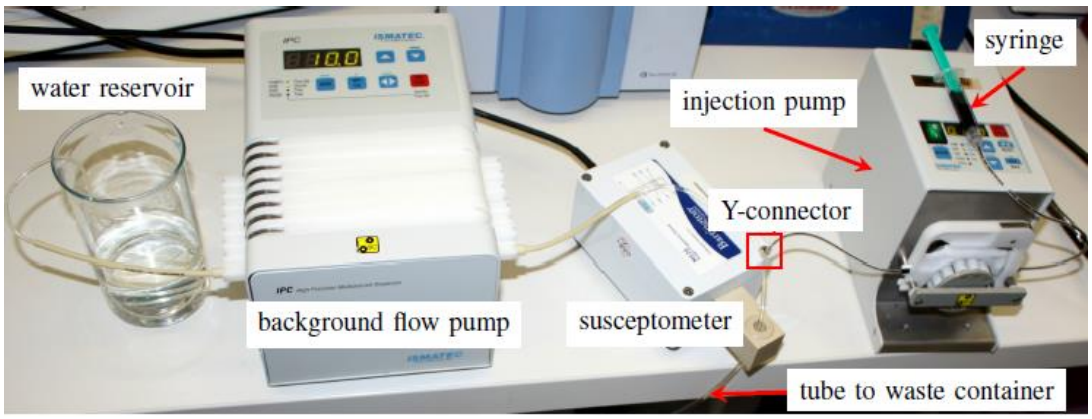

Figure 3.1: Photograph of the molecular communication system developed by FAU [2].

The particles are stored in a syringe together with water. This syringe is connected via a tube with an electronic pump (Ismatec® Reglo Digital, Germany), which controls the

injection of the mixture through another tube with a constant flow rate and injecting a dosage volume of few microliters of particle suspension. This tube concludes in a Y-connector, where a second tube is connected (see Figure 3.2). A second pump (Ismatec® IPC, Germany) provides a constant background flow of water through this last tube for signal propagation. At the exit of the Y-connector, it is placed the propagation channel, through which the sum of particle suspension and background flow is transmitted.

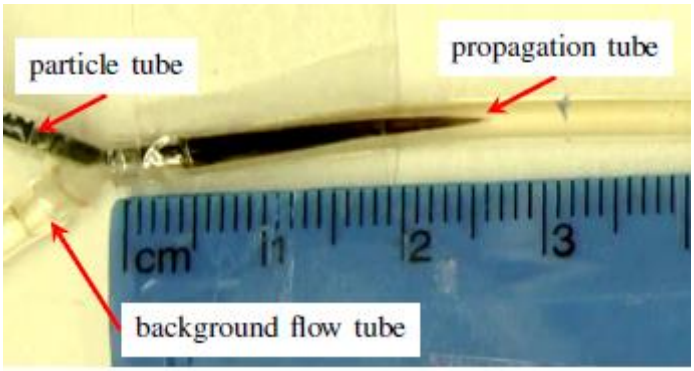

Figure 3.2: Photograph of the Y-connector. The particle tube and the background flow tube are placed in the entrance of the splitting, whereas the propagation tube in its exit [2].

For signal reception, it is employed a susceptometer (MS2G Bartington®) at the end of the propagation channel, an electronic device including a coil, where the magnetic particles move through and generate an electrical signal $\chi(t)$ proportional to the quantity of magnetic particles flowing in that area; it measures susceptibility changes. This changes are monitored and recorded with the software Bartsoft (Bartington Instruments, Witney, UK). Finally, the mixture of SPIONs and water is collected in a waste container.

The system is able to send text messages as encoded bits by SPIONs according to the next procedure: using a custom LabVIEW (National Instruments, Austin, Texas, USA) graphical user interface (GUI), the first pump mentioned in this chapter switches the injection of SPIONs into the propagation channel. When a dose of particle solution arrives at the susceptometer, then the susceptibility change is interpreted as a bit ”1”; when no particles are registered in the receiver, then it is interpreted as a bit ”0”. The synchronization is accomplished using the 8 bit extended ASCII encoding for capital letters, which is composed of 26 capital letters with a [0, 1, 0] prefix: when the susceptometer detects the first peak, which belongs to the bit ”1” of the prefix, then the start of a character is recognised.

The goal of this work is to optimize the transmitter of this setup using an electromagnet near the area of the Y-connector in order to steer the SPIONs to a desired path after the splitting. In next section, the method accomplished for this purpose is described.

Chapter 4

Optimization of the Current System

Now that we know how the current system developed by FAU works, a modification of it is proposed in order to optimize the transmitter. The aim is to steer the SPIONs through a desired tube under the influence of a magnetic field. For that purpose, an electromagnet is used. In the following, a detailed description of the circuit used to control the switch of the electromagnet is presented, as well as the whole testbed used during the experiments.

4.1 Testbed to Steer the SPIONs

A schematic of the testbed proposed to study the efficacy of the magnetic field generated by the electromagnet on SPIONs is shown in Figure 4.1.

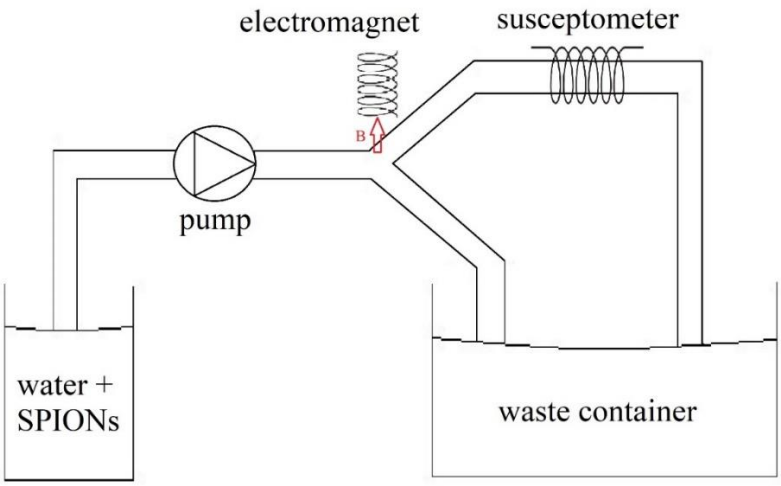

Figure 4.1: Schematic representation of the testbed proposed to check the efficacy of a magnetic field on SPIONs.

The mixture of water and SPIONs is pumped by a peristaltic pump towards the Y-connector with a constant flow. Near the split an electromagnet is placed, so that its magnetic field steers the magnetic particles through the propagation channel, where the susceptometer works as receiver of the system. The aim is to attract the maximum SPIONs towards the susceptometer in order to get a good signal reception. Finally, the mixture is collected in a waste container.

Next, the chosen electromagnet and the electronic circuit that controls its switch is presented.

4.1.1 Electromagnet

An electromagnet ITS-MS-2015 from the manufacturer Red Magnets has been selected, due to its small size and voltage supply rate (see Table 4.1). Including its external case, it has a diameter of 20 mm and a length of 15 mm, which makes it appropriate to use with the testbed. We try to use an electromagnet whose size do not exceed very much the size of the tubes used in the testbed, since it will be placed near them.

Table 4.1: ITS-MS-2015 electromagnet parameters. Information provided in the datasheet of the component and by the manufacturer.

Parameter	**Numerical Value**
Length	15 mm
Diameter	20 mm
Number of turns N	1000
Series resistance R_{DC}	66 Ω
Inductance	57 mH
Maximum voltage supply	12 V
Maximum power dissipation	2 W
Maximum force	20 N

The electromagnet contains a core composed of 12L12 carbon steel and has a number of turns of 1000. Its DC resistance is 66 Ω, it can be supplied with a maximum DC voltage of 12 V and it can dissipate a maximum power of 2 W.

In order to see if the SPIONs are attracted by the magnetic force generated by the electromagnet, the next quick test has been made: a small plastic glass has been filled

with a mixture of SPIONs and water, near of which the component has been located, see Figure 4.2.

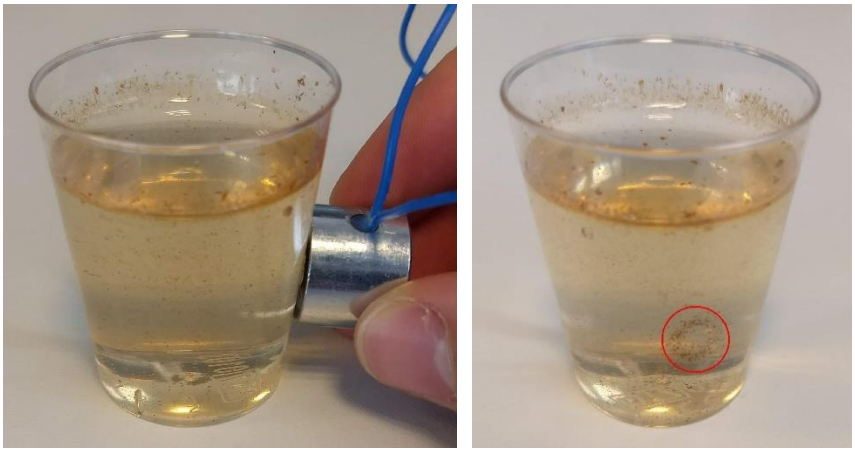

(a) (b)

Figure 4.2: (a) Activated electromagnet near a plastic glass with a mixture of SPIONs and water; (b) Agglomerated SPIONs (red circle) in the area where the electromagnet was placed.

The electromagnet has been sourced with a range voltage of 0 – 11 V. It has not been supplied with 12 V (the maximum allowed), since it exceeds its maximum power dissipation of 2 W (determined with the simulation software LTspice®). Thus, a series resistance *R* with the electromagnet would be required for that situation.

When the electromagnet, which is represented by a coil in the schematic of Figure 4.3, works with DC, it behaves as a wire with a resistance equivalent to R_{DC}.

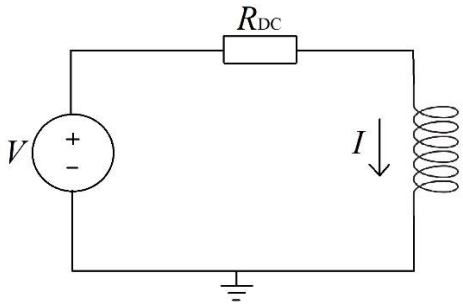

Figure 4.3: Schematic of an electromagnet supplied with a DC voltage source *V*.

According to Ohm's law, the maximum current flowing through the component is:

$$I = \frac{V}{R_{DC}} = \frac{11\ V}{66\ \Omega} = 0.167\ A \tag{4.1}$$

As Figure 4.2 shows, the SPIONs are attracted and they agglomerate in the area where the electromagnet has been placed, which implies that it should work in the testbed of Figure 4.1.

In next section, the electronic circuit designed to control the switch of the electromagnet is shown.

4.1.2 Control Circuit to Switch the Electromagnet

To switch the electromagnet, the electronic circuit shown in Figure 4.4 is used.

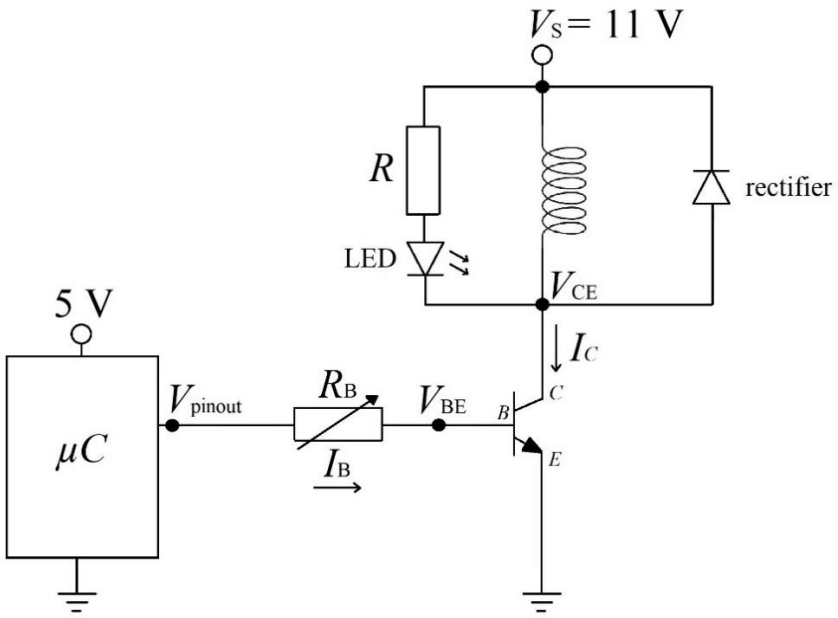

Figure 4.4: Schematic of the electronic circuit used to control the switch of the electromagnet.

The circuit is controlled automatically by a microcontroller, which gives a high output voltage signal (5 V) or a low one (0 V) according to its programming. When this signal is high, the BJT transistor works in saturation mode allowing the current conduction I_C from the collector (*C*) to the emitter (*E*), thus, the electromagnet is activated; when the signal is low, the BJT works in cut-off mode, with the result that I_C is zero and the electromagnet is deactivated. Summarizing, the transistor works as a switch whose state (open or closed) depends on the signal coming from the microcontroller.

The microcontroller is supplied with a fixed 5 V voltage source, whereas the electromagnet is supplied with a variable one, from 0 to 11 V, in order to get different I_C

and thus, different magnetic forces generated by the electromagnet that are used during the experiments with the testbed. For this reason, a potentiometer has been selected as the base resistance (R_B) of the transistor; different values of voltage supply on the electromagnet require different values of R_B, and a potentiometer is an easy option to get it.

The circuit also includes a resistor (R) and a LED, which illuminates when the electromagnet is switched on; it is only an informative indication. The electromagnet has also parallel a rectifier diode in order to protect the transistor from the high peaks generated by the electromagnet when it switches off. When it occurs, the flowing current through the coil is quickly interrupted and the magnetic field present in it induces, for a brief moment, a very high voltage of opposite polarity in its terminals, which could damage the BJT. The rectifier absorbs this peak voltage.

In Figure 4.5, the circuit mounted on a protoboard is shown. The different electronic components that compose the circuit are described next with the exception of the electromagnet, which is already explained in section 4.1.1.

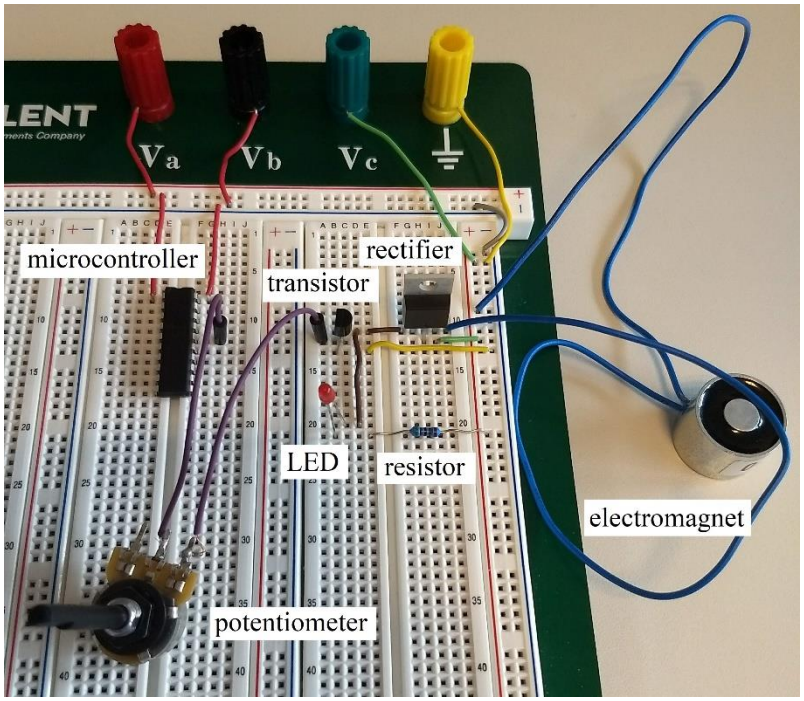

Figure 4.5: Electronic circuit to control automatically the switch of the electromagnet mounted on a protoboard.

4.1.2.1 Microcontroller

The microcontroller selected is the PIC16F690, which belongs to family PIC from the manufacturer Microchip Technology. It has been chosen this microchip because it meets the requirements demanded by the system. Moreover, it is very economical and contains a big range of functions that facilitate its programming. Figure 4.6 shows its pin diagram.

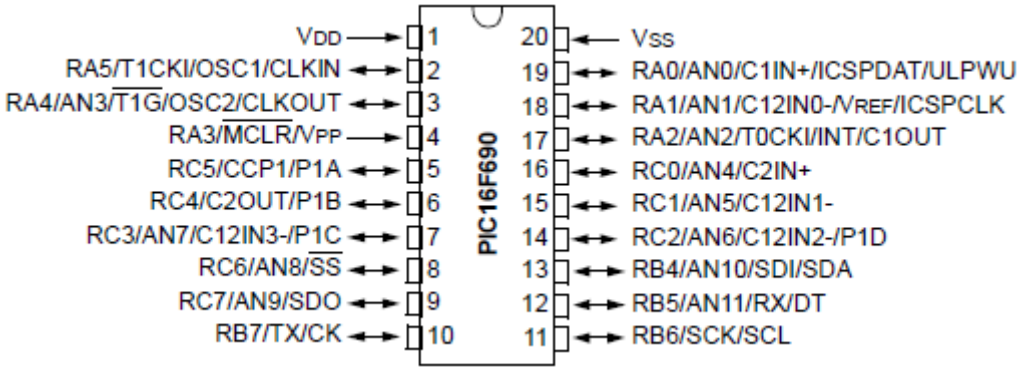

Figure 4.6: PIC16F690 pin diagram [17].

It must be supplied with 5 V by pins 1 and 2, which are the high voltage and ground, respectively. In this work, only the pinout RC0 (pin number 16) is used to transfer the information to the transistor. Therefore, the mentioned pin will be approximately at 5 V during the switch on of the electromagnet. The maximum value of output current sourced by the pin is 25 mA.

The programming code of the microcontroller has been done with version 4.20 of the editor MPLAB X IDE (Microchip Technology Inc., Chandler, Arizona, USA), which is destined to products from Microchip. This editor is based on *c* programming language to make the code. To compile it, which means to transform the commands that constitute the program from *c* programming language to machine language (binary code), the version 2.0 of the compiler XC8 (Microchip Technology Inc., Chandler, Arizona, USA) has been used. Finally, the program has been transferred from the computer to the microcontroller with a programmer device PICkit 3.

Programming code

Figure 4.7 shows two examples of the programming code used in this thesis for the microcontroller. The first two lines are included, so that MPLAB and the compiler XC8 load automatically the registers and parameters of the PIC16F690. In this way, when we

write in the code the name of a pin, a bit or a register of the microchip, it is automatically identified.

```
1  #include <xc.h>
2  #include <pic16f690.h>
3
4  #pragma config FOSC = INTRCIO
5  #pragma config WDTE = OFF
6  #pragma config PWRTE = OFF
7  #pragma config MCLRE = OFF
8  #pragma config CP = OFF
9  #pragma config CPD = OFF
10 #pragma config BOREN = OFF
11 #pragma config IESO = OFF
12 #pragma config FCMEN = OFF
13
14 #define _XTAL_FREQ 4000000
15
16 void main(void)
17 {
18     TRISC = 0b11111110;
19
20     while(1)
21     {
22     PORTCbits.RC0 = 1;
23     }
24 }
```

(a)

```
1  #include <xc.h>
2  #include <pic16f690.h>
3
4  #pragma config FOSC = INTRCIO
5  #pragma config WDTE = OFF
6  #pragma config PWRTE = OFF
7  #pragma config MCLRE = OFF
8  #pragma config CP = OFF
9  #pragma config CPD = OFF
10 #pragma config BOREN = OFF
11 #pragma config IESO = OFF
12 #pragma config FCMEN = OFF
13
14 #define _XTAL_FREQ 4000000
15
16 void main(void)
17 {
18     TRISC = 0b11111110;
19
20     while(1)
21     {
22     PORTCbits.RC0 = 1;
23     __delay_ms(1000);
24     PORTCbits.RC0 = 0;
25     __delay_ms(1000);
26     }
27 }
```

(b)

Figure 4.7: Examples of the programming code used to control the switch of the electromagnet; both codes are done with the editor MPLAB X IDE, version 4.20. (a) shows the programming code to switch the electromagnet on indefinitely; (b) shows the programming code to switch it on/off with a period of 1 s (0.5 seconds on and 0.5 seconds off).

Next, we must configure the configuration bits of the PIC (see lines 4 to 12 of Figure 4.7), which are related to general working modes of the microcontroller such as a start timer (bit PWRTE), restarting in case of supply lost (bit BOREN), etc. All of them are deactivated (OFF) because they are not relevant for the good operation of the control circuit, with the exception of the bit FOSC. This is the bit to select the type of frequency oscillator, which has been configured as inner (INTRCIO) in such a way it is not required an external electronic circuit to generate this timing signal. The frequency oscillator is the

circuit that indicates the speed with which the microcontroller works, and thus, it is an essential component of all microprocessors or microcontrollers. It is a timing signal that specifies the execution time of a programming instruction. Every four cycles or periods (*T*) of this signal, an instruction of the programming code is executed. Therefore, if the frequency (*f*) is configured as 4 MHz (see line 14 in Figure 4.7), each instruction will be executed in 1 µs:

$$\frac{time}{instruction} = 4 \cdot T = 4 \cdot \frac{1}{f} = 4 \cdot \frac{1}{4 \cdot 10^6\ s^{-1}} = 10^{-6}\ s = 1\ \mu s \qquad (4.2)$$

After the configuration of the bits and the definition of the frequency oscillator, comes the main program. In line 18, the pin RC0 of the microcontroller is configured as an output pin, since we use it to control the switch of the electromagnet. After that, Figure 4.7 shows two alternatives: (a) switches the electromagnet on indefinitely; (b) switches it with a period of 1 s (0.5 seconds on and 0.5 seconds off). During testing of the circuit together with the rest of the setup we will test both programs. Also we will check different values of switch period.

4.1.2.2 Transistor

Taking into account the maximum collector-emitter voltage (V_{CE}) at which the transistor will be subjected and the maximum current (I_C) that will flow through the electromagnet, which are approximately 11 V and 167 mA, a transistor BC337-40 of type npn has been chosen. It tolerates a maximum V_{CE} of 45 V and a maximum I_C of 800 mA.

4.1.2.3 Rectifier Diode

The model selected as rectifier diode is the SDT20120CT, with a maximum DC blocking voltage (V_{RM}) of 120 V and an average rectified output current (I_O) of 20 A. This values guarantee the good work of the component. The rectifier is connected parallel with reversed polarity to the electromagnet in order to allow the flowing of current when the transistor switches off. When it occurs, a very high voltage of opposite polarity is generated in the terminals of the electromagnet. Thus, the rectifier absorbs this voltage peak and protects the transistor.

4.1.2.4 LED and Resistor

As informative indication of the activation of the electromagnet, a general red LED with a DC forward current value (I_F) of 2 mA and a forward voltage of 1.6-2 V has been integrated in the circuit. A resistor of 500 Ω has been arranged in series with the LED in order not to surpass its $I_{F\,max}$, which has a value of 30 mA.

4.1.2.5 Potentiometer

In the circuit, a potentiometer works as base resistance (R_B) of the BJT, which allows to modify its resistance value according to the circuit necessities. These requirements are the different values of I_C that are needed in order to get different values of magnetic force generated by the electromagnet. We want to test this circuit with the proposed testbed of Figure 4.1, trying different values of magnetic force in order to check which one steers the SPIONs most effectively.

To calculate R_B, we need to know I_C, which is the sum of the current flowing through the electromagnet plus the current flowing through the LED. This last current has an approximately value of 2 mA (typical I_F of the LED), much lower than the first one, thus, it is considered negligible. I_C is, then, the current flowing through the electromagnet. Knowing that its R_DC has a value of 66 Ω and employing Ohm's law, we obtain different values of I_C according to the voltage V_S used to source the electromagnet:

$$I_\mathrm{C} = \frac{V_\mathrm{S}}{R_\mathrm{DC}} \tag{4.3}$$

Next, the DC current gain (β) of the transistor is determined with a multimeter. It has a value of 307 (dimensionless in SI units). Therefore, the current flowing through the base of the transistor I_B is:

$$I_\mathrm{B} = \frac{I_\mathrm{C}}{\beta} = \frac{I_\mathrm{C}}{307} \tag{4.4}$$

I_B is also the current flowing through the pinout of the microcontroller, which can have a maximum value of 25 mA. If it is exceeded, the PIC could be damaged. As a protection measure, the value obtained with equation 4.4 is multiplied by a security factor of 5. Finally, the value of R_B can be calculated using Ohm's law:

$$R_{\mathrm{B}} = \frac{V_{\mathrm{B}}}{I_{\mathrm{B}}}$$

$$R_{\mathrm{B}} = \frac{V_{\mathrm{pinout}} - V_{\mathrm{BE}}}{I_{\mathrm{B}}} \tag{4.5}$$

$$R_{\mathrm{B}} = \frac{5\ \mathrm{V} - 0.7\ \mathrm{V}}{I_{\mathrm{B}}}$$

where V_{pinout} is the voltage of the pinout of the microcontroller (approximately 5 V) and V_{BE} is the base-emitter voltage, which is 0.7 V due to the transistor is made of silicon. The results are shown in Table 4.2.

Table 4.2: Acquired values for the collector current I_{C} and base current I_{B} according to the voltage supply of the electromagnet V_{S}. Also the value of the base resistor R_{B} that is required for each situation. I_{C}, I_{B} and R_{B} are calculated with equations (4.3), (4.4) and (4.5), respectively.

V_{S} [V]	I_{C} [mA]	$I_{\mathrm{B}} \cdot 5$ [mA]	R_{B} [Ω]	commercial R_{B} [Ω]
1	15	0.25	17425.3	18k
2	30	0.49	8712.7	8200
3	45	0.74	5808.4	5600
4	61	0.99	4356.3	4700
5	76	1.23	3485.1	3300
6	91	1.48	2904.2	2700
7	106	1.73	2489.3	2700
8	121	1.97	2178.2	2200
9	136	2.22	1936.1	1800
10	152	2.47	1742.5	1800
11	167	2.71	1584.1	1500

As we can see, the I_{B} acquired (multiplied by a security factor 5) is lower than the maximum allowed in the pinout of the microcontroller (25 mA). The values of R_{B} calculated with equation (4.5) have been rounded to values of commercial resistors, so that it is easier to adjust the potentiometer. Furthermore, if it is desired in the future to use the circuit with only a specific voltage supply of the electromagnet, then the potentiometer can be replaced by a commercial resistor whose value is indicated in the table.

It is considered that with 1 V the electromagnet will do no effect on the magnetic particles due to a low magnetic force. Thus, neglecting the value of 18 kΩ, it is needed a potentiometer that covers a value of resistance from 1500 to 8200 Ω. It has been selected a general one with a maximum value of 10 kΩ.

4.1.3 Simulation of the Control Circuit

The circuit presented in the previous section has been simulated with the different values of voltage source V_S and commercial R_B shown in Table 4.2. As Figure 4.8 shows, the microcontroller is replaced by a DC voltage source of 5 V in the simulation, since this is the value it gives approximately in its pinout. The LED and resistor *R* have been not taken into account because they are only used as an informative indication and do not affect the proper operation of the circuit. For that purpose, it has been used the simulation software LTspice® (Linear Technology).

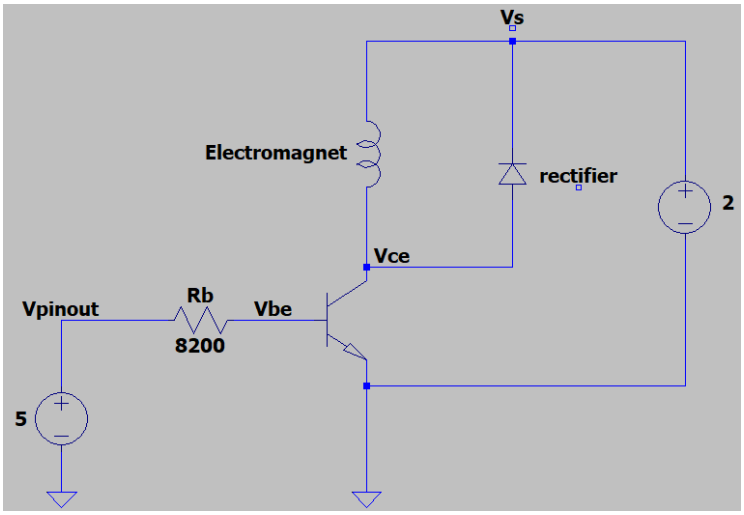

Figure 4.8: Electronic circuit simulated with LTspice. In this case, the electromagnet is sourced by 2 V and the base resistor is 8200 Ω, as it is denoted in Table 4.2.

The results of the simulation, when the transistor works in saturation mode, are shown in Table 4.3. The simulation has yielded good results: the base current I_B does not exceed the maximum allowed by the pin of the microcontroller (25 mA); the current through the electromagnet I_C coincides with little error (less than 8%) with the one calculated previously and showed in Table 4.2; the voltage between the base and the emitter of the transistor V_{BE} is more than 0.7 V (condition required to work in saturation mode).

Table 4.3: Acquired values from the simulation when the transistor works in saturation mode (switched on), according to the voltage supply of the electromagnet V_S: the collector current I_C, the base current I_B, the collector-emitter voltage V_{CE} and the base-emitter voltage V_{BE}.

V_S [V]	I_C [mA]	I_B [mA]	V_{CE} [mV]	V_{BE} [V]
2	28.63	0.50	110.63	0.86
3	43.76	0.74	112.04	0.87
4	58.85	0.88	115.95	0.88
5	74.06	1.25	112.06	0.89
6	89.22	1.52	111.65	0.89
7	104.29	1.52	116.65	0.90
8	119.48	1.86	114.46	0.90
9	134.67	2.28	111.93	0.90
10	140.77	2.28	115.31	0.90
11	164.96	2.73	112.61	0.91

4.1.4 Testing of the Control Circuit

Next step is doing testing with the designed circuit. For that purpose, the testbed shown in Figure 4.9 has been used. We want to check the proper operation of the circuit for each voltage value that sources the electromagnet.

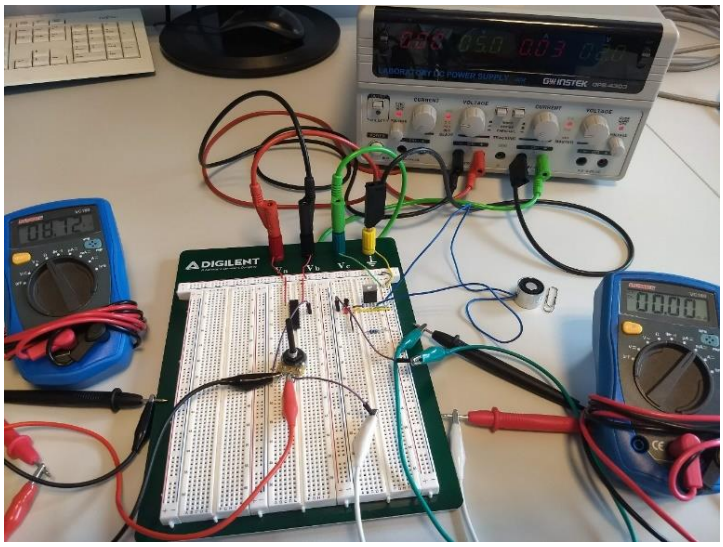

Figure 4.9: Testbed used to check the functioning of the control circuit to switch the electromagnet.

The circuit has been tested with a cyclical switch of 8 seconds (4 seconds on and 4 seconds off), but only the results when the transistor is working in saturation mode (switched on) are presented in Table 4.4. When the transistor works in cut-off mode (switched off), no current flows through the electromagnet, thus, no magnetic force is generated. It has been checked that the rectifier works properly and absorbs the voltage peak produced by the electromagnet when it is switched off almost immediately.

Table 4.4: Acquired values from the testing when the transistor works in saturation mode (switched on), according to the voltage supply of the electromagnet V_S: the voltage of the pinout of the microcontroller V_{pinout}, the collector current I_C, the base current I_B, the collector-emitter voltage V_{CE} and the base-emitter voltage V_{CE}.

V_S [V]	V_{pinout} [V]	I_C [mA]	I_B [mA]	V_{CE} [mV]	V_{BE} [V]
2	5.00	28.19	0.52	51.75	0.71
3	4.98	41.70	0.75	59.20	0.73
4	4.97	55.60	0.90	70.07	0.74
5	4.95	69.50	1.27	73.30	0.75
6	4.94	83.90	1.54	82.34	0.76
7	4.94	95.40	1.54	94.30	0.76
8	4.92	110.40	1.87	97.88	0.77
9	4.90	122.40	2.27	104.30	0.78
10	4.90	133.80	2.28	112.10	0.78
11	4.88	148.70	2.70	118.34	0.79

As we can see in the table above, the output voltage sourced by the microcontroller in its pinout keeps approximately 5 V for each value of V_S. The obtained base current I_B is much less than 25 mA (the maximum allowed) and differs maximum a 4% from the one obtained in simulation; the collector current differs less than 10%. These results are good, since we had applied a security factor of 5 when we have determined the values of the base resistor (potentiometer) in section 4.1.2.5 of this document. Therefore, there is a big margin of error. Furthermore, acquired values of V_{CE} and V_{CE} confirm that the transistor is working properly in saturation mode. The LED emits light for each situation of the table and the electromagnet attracts a paperclip when is switched on, thus, it is confirmed that a magnetic force is generated.

In next section, the electronic circuit is tested together with the molecular testbed developed by FAU in order to check if the electromagnet affects the SPIONs trajectory

Chapter 5

Results and Discussion

After having confirmed that the designed circuit to control the switch of the electromagnet works properly, it has been tested together with the rest of the setup. Two rounds of testing have been conducted: the first one without susceptometer in order to acquire a qualitative view of the efficacy of the electromagnet in the system operation; a second one with susceptometer in order to obtain accurate results.

5.1 Testing without Susceptometer

The whole testbed we want to test, which is showed in Figure 4.1 from section 4.1, contains many variables that could affect the behaviour of the SPIONs whereas they are flowing in the system. These variables are the voltage source of the electromagnet (V_S), the switch period of the electromagnet (*T*, configured in the programming code), the flow rate pumped (Q), the position of the electromagnet in the testbed, and the ratio SPIONs and water used in the injected mixture.

A first round of testing has been accomplished, in which the susceptometer has not been used (see Figure 5.1). Because of that, we can not determine with accuracy if more magnetic particles are steered through the desired path after the Y-connector due to the influence of the electromagnet, but we acquire a qualitative view of the general operation of the system.

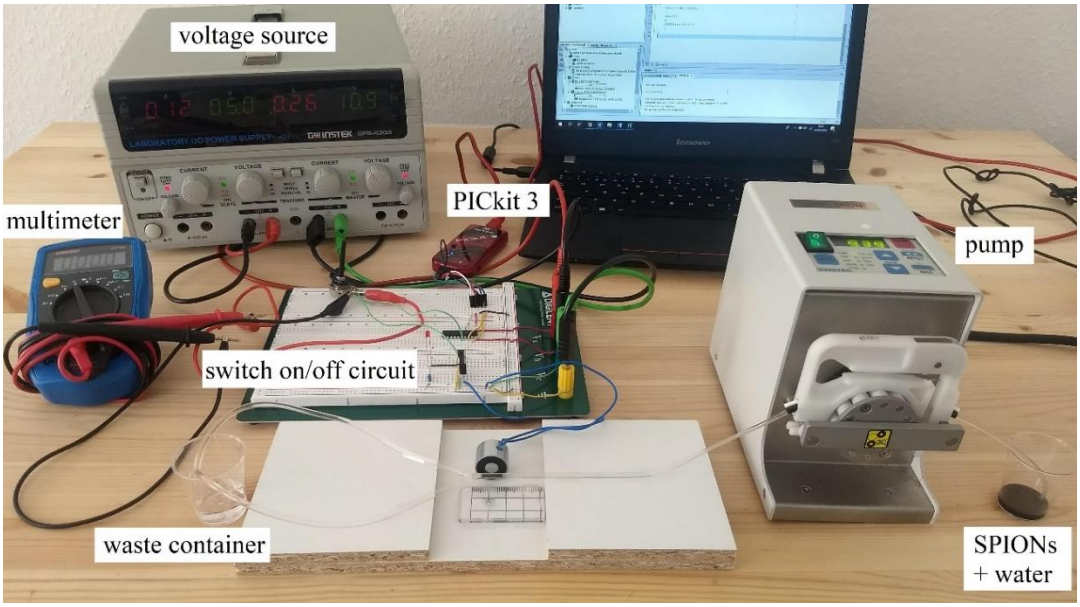

Figure 5.1: Testbed used for experiments without susceptometer.

For this testing, the mixture of SPIONs and water has been fixed as 1 mL of SPIONs plus 1 mL of water in order not to have many variables. This mixture is pumped towards the Y-connector, near which the electromagnet is located. Finally, the particles and water are collected in a waste container.

For the electromagnet positioning, two rulers with cm scale have been incorporated, being the position (x, y) = (0, 0) the beginning of the split (see Figure 5.2). The electromagnet is also placed in such a way that its longitudinal axis crosses the tubes where the SPIONs are flowing.

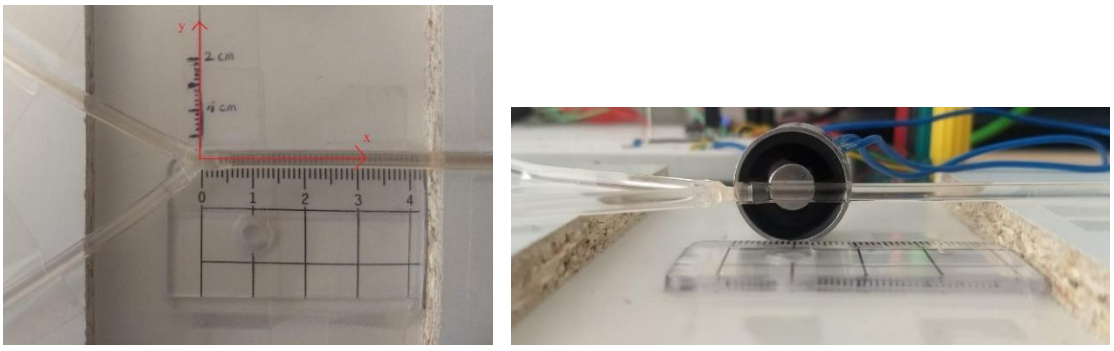

(a) (b)

Figure 5.2: (a) Rulers with cm scale to reference the location of the electromagnet in the testbed. Position (x, y) = (0, 0) is the start of the Y-connector. (b) Front view of the electromagnet located in the setup.

A multimeter has been used to verify the resistance value selected with the potentiometer (R_B). Since it is a handmade operation and it is difficult to get an identical value as the indicated in Table 4.2 (commercial R_B), we consider good resistance values those with a margin of ±10 Ω. Thus, if the value of R_B must be 1500 Ω, but we get one of 1490 or 1510 Ω with the potentiometer, then it is considered correct. It is reasonable since we have applied a security factor of 5 when we have determined the required values of base resistor according to the voltage supply of the electromagnet in section 4.1.2.5, thus, it does not affect the proper working of the control circuit of the electromagnet.

In this testing several values of the different variables of the system has been used:

- The next pumped flow rates Q in mL/min: 0.5, 1, 2, 3 and 4.
- The next positions (x, y) in cm for the electromagnet: (1, 0), (1.5, 0), (2, 0) and (0, 0.7) being x the position of the longitudinal axis of the component.

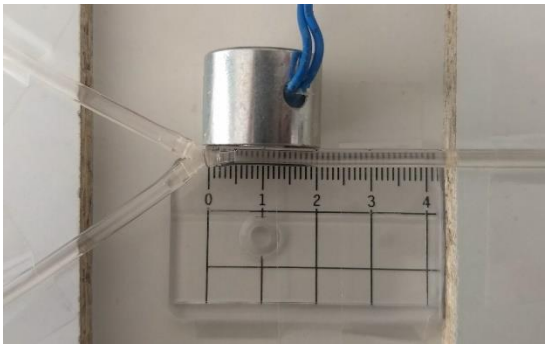

Figure 5.3: Electromagnet in position (1,0) cm.

- The next voltage sources of the electromagnet V_S in volts: 2, 3, 4, 5, 6, 7, 8, 9, 10, 11.
- The next switch periods *T* of the electromagnet in seconds: 0.1, 0.5, 1, 2, 4. Also, it has been tested with the electromagnet switched on indefinitely.

As illustrated in Figure 5.4, the mixture of SPIONs and water flow through both channels after the Y-connector without the influence of a magnetic field generated by the electromagnet.

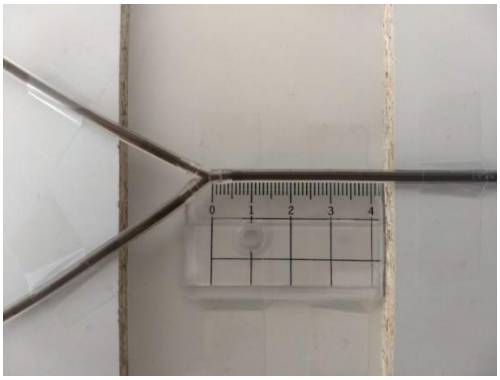

Figure 5.4: Testbed working without the electromagnet. As a result, the mixture of SPIONs and water flows through both channels after the Y-connector.

First, it has been tested with the electromagnet switched on indefinitely and different combination of the rest of variables. In all cases, it has been observed the same performance: when the mixture arrives at the area where the electromagnet is located, the particles are attracted to the walls of the tube (see Figure 5.5) and then, they start to flow through the desired path (correct path) after the Y-connector.

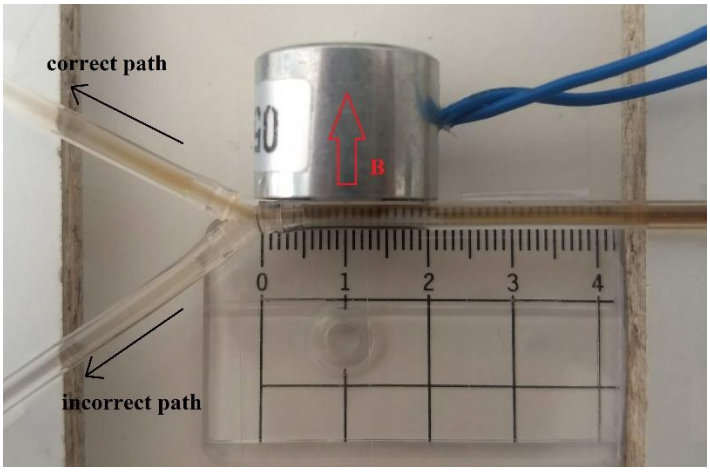

Figure 5.5: Mixture flowing through the desired path after the Y-connector. It can be appreciated how the SPIONs are attracted to the border of the tube near the electromagnet. Flow rate Q = 0.5 mL/min; voltage source of the electromagnet V_S = 11 V; electromagnet in position (1,0) cm; electromagnet switched on indefinitely.

After some seconds, it seems they agglomerate near the electromagnet, which block the proper flow through the correct path and they begin to flow in both channels (see Figure 5.6).

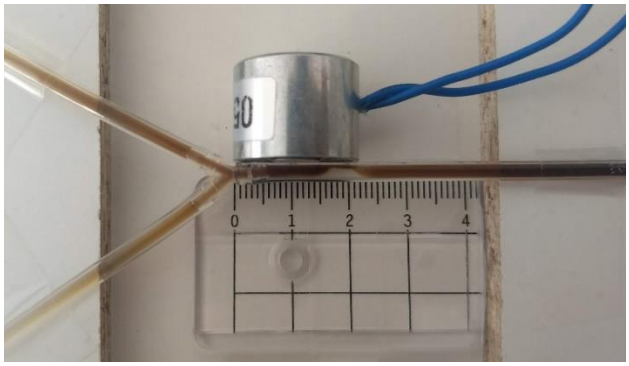

Figure 5.6: Mixture flowing through both channels after the Y-connector. Flow rate Q = 0.5 mL/min; voltage source of the electromagnet V_S = 11 V; electromagnet in position (1, 0) cm; electromagnet switched on indefinitely.

After the particles have started to flow through the desired way, the maximum time it takes to them to start to flow through both channels (*t*) is approximately 30 seconds, for a flow rate Q of 0.5 mL/min. This time decreases as greater is Q, obtaining one of approximately 8 seconds for a flow rate of 4 mL/min and sourcing the electromagnet with 2 V. Placing the electromagnet in position (0, 0.7) cm (see Figure 5.7), (1.5, 0) cm or (2, 0) cm, acquired results are worse (shorter *t*).

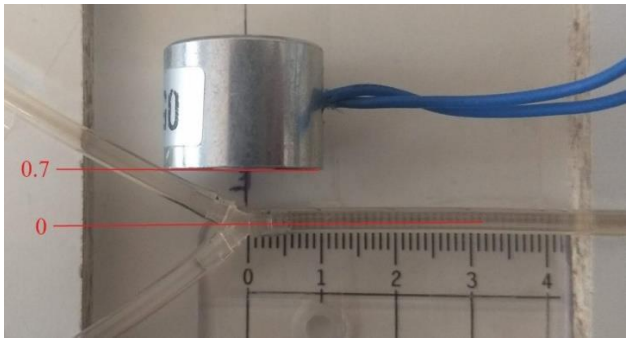

Figure 5.7: Electromagnet in position (0, 0.7) cm.

Finally, it has been observed the shorter the switch period of the electromagnet is, better results are acquired (greater *t*). It could be on account of a less agglomeration of the particles (during the switch on, the electromagnet attracts the particles; during the switch off, they flow freely). The best obtained results are with a switch period of 200 ms (100 ms on and 100 ms off, cyclically). In this situation, the greatest *t* is 1 min for a flow rate of 0.5 mL/min.

Thus, for the moment, we can conclude that the best position of the electromagnet to work more effectively is (1, 0) cm; the lower is the flow rate Q, better results are acquired and short switch periods of the electromagnet are better. Anyway, these results are qualitative since a susceptometer has not been used. In next section, accurate results of testing using this device are presented.

5.2 Testing using a Susceptometer

In next testing, a MS2G Bartington® susceptometer coil (inner diameter: 10 mm, height: 5 mm) has been employed in order to determine with precision the effectiveness of the magnetic field on SPIONs. A susceptometer is an electronic device including a coil, where the magnetic particles move through and generate an electrical signal χ(t). This signal is proportional to the number of SPIONs that are within the detection range at a specific time instance. Susceptibility changes measured are recorded by use of the software Bartsoft 4.2.1.2 (Bartington Instruments, Witney, UK) provided by the manufacturer of the susceptometer. For that purpose, the testbed shown in Figure 5.8 has been used.

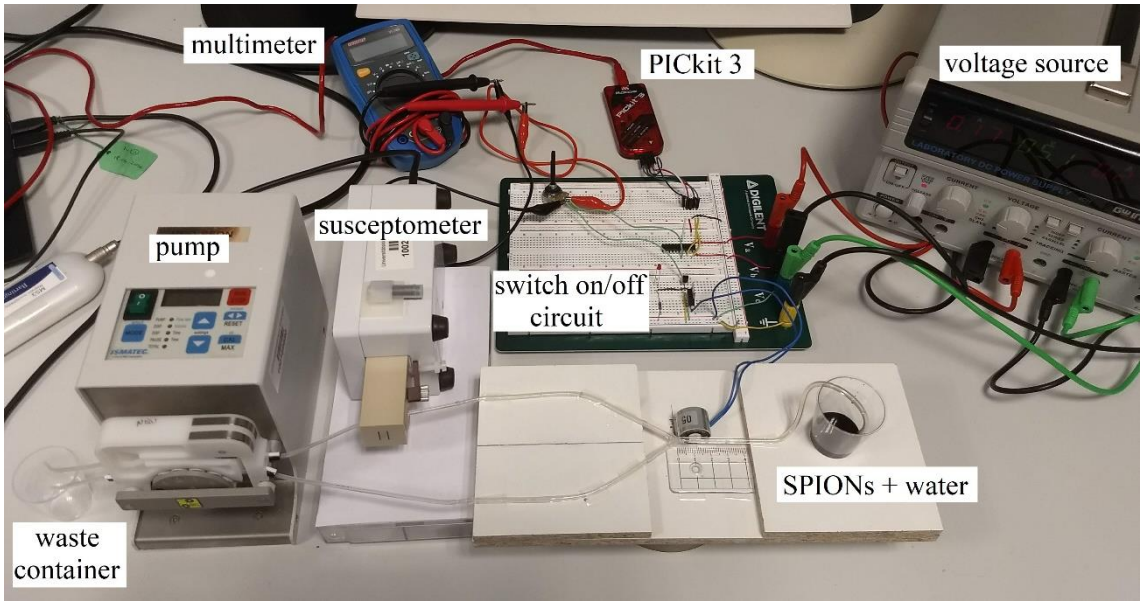

Figure 5.8: Testbed used to check the efficacy of the magnetic field generated by an electromagnet to steer SPIONs through a molecular communication system.

All tubes have an inner diameter of 0.8 mm, both channels after the Y-connector have the same length and are positioned symmetrically.

In order to guarantee equal flow conditions in both channels after the splitting, two pumps in parallel have been used, one for each channel. The two pieces shown in Figure 5.9 have been used to get identical parallel flows with the same pump. In this way, the flow rate acquired in the tube placed between the glass with SPIONs and the start of the splitting

(flow rate Q), is the sum of the flow rates of both channels after the Y-connector.

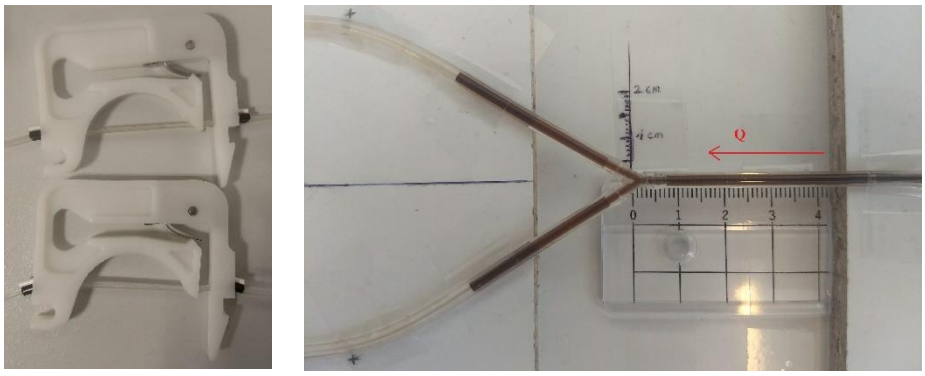

(a) (b)

Figure 5.9: (a) Pieces used to get equal parallel flows in both channels after the Y connector. (b) Photograph where we can see how the mixture flows at the same time through both ways.

The purpose is to measure the magnetic susceptibility of both paths after the Y-connector in order to see if there is a difference between them. In particular, a greater value in the desired path than the other one is expected, since more SPIONs in the first way are supposed to flow due to the influence of the magnetic field.

The ideal would be to use two susceptometers, so that the magnetic susceptibilities of both channels were measured at the same time. Nevertheless, FAU can only provide one device. For that reason, the next procedure has been accomplished:

1. First, the magnetic susceptibility has been measured without using the electromagnet in the system. In this way, a baseline is acquired. For this operation, the susceptometer can be placed in any of two channels, since there is no magnetic field generated and, thus, SPIONs flow equally through both tubes (see Figure 5.10).

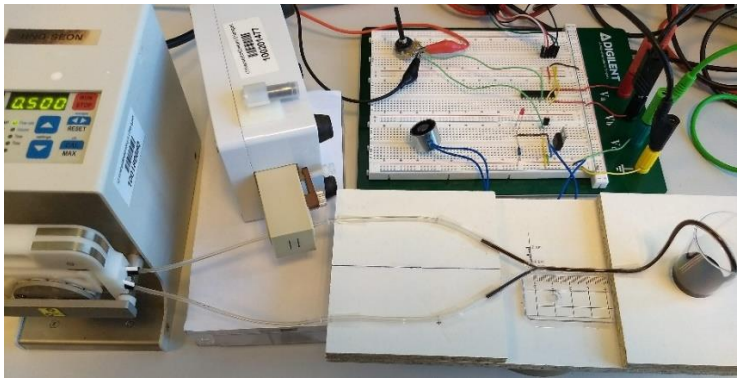

Figure 5.10: Susceptometer positioned in one of the channels in order to acquire a magnetic susceptibility baseline. For this operation the electromagnet is not used.

2. Next step is activating the control circuit of the electromagnet and measuring of magnetic susceptibility in one of the channels, as illustrated in Figure 5.11.

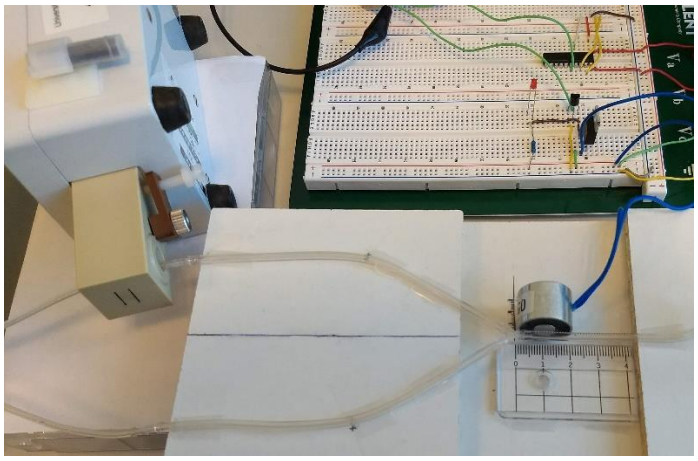

Figure 5.11: Measuring of magnetic susceptibility changes in one of the channels with the electromagnet activated. In this case, the device is positioned in the desired path (correct path), where the SPIONs are supposed to flow with larger proportion than in the other path (incorrect path) due to the effect of the magnetic field.

3. Finally, measuring of magnetic susceptibility changes in the other channel are registered, being also the electromagnet switched on.

In steps 2 and 3, the susceptometer has been placed at the same areas in respective channels, so that the measuring conditions were as similar as possible. Also, the start of each measuring round has been done as soon as the mixture of SPIONs and water reaches the red line shown in Figure 5.12.

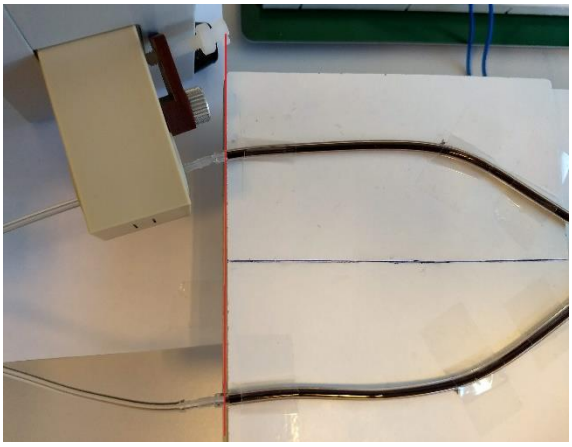

Figure 5.12: Susceptometer location in the testbed. When the particles reach the red line, then the susceptometer start to measure the magnetic susceptibility changes.

A total number of 1000 samples every 0.1 seconds (in total, 100 seconds) have been registered for each measurement round. Finally, after the particles have passed through the susceptometer and the pump, they are collected in a waste container in order to be reused.

The next values for the different variables of the system have been used:

Table 5.1: Values of the different variables that have been tested during experiments with the setup using a susceptometer.

Variable	**Values**
Flow rate Q [mL/min]	0.752, 1, 2, 3, 4
Electromagnet voltage source V_s [V]	2, 6, 11
Electromagnet position (x, y) [cm]	(1, 0), (1.5, 0), (0, 0.8)
Electromagnet switch period T [s]	0.01, 0.1, 0.5, 2
Mixture (mL SPIONs, mL water)	(1, 2), (1, 4)

SPIONs with a hydrodynamic particle radius of 27.5 nm are used. The electromagnet positions indicated in the table above are shown in Figure 5.13, being the position (0, 0) the start of the Y-connector; x coordinate corresponds to the longitudinal axis position of the electromagnet; y coordinate is the position of the electromagnet front face.

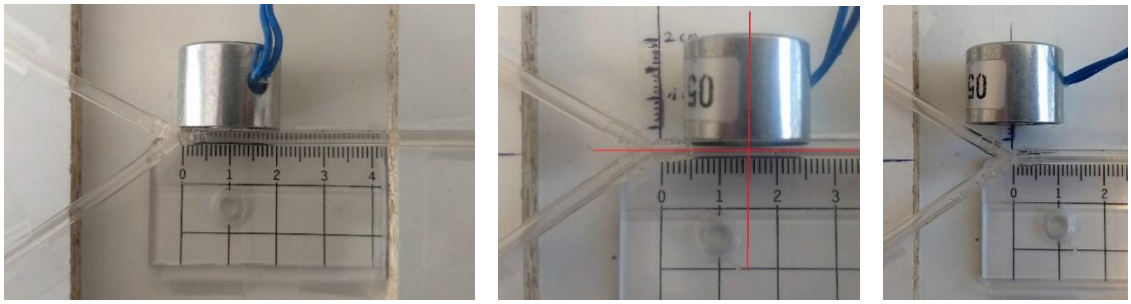

(a) (b) (c)

Figure 5.13: Electromagnet positions tested during experiments with susceptometer. x coordinate is the position of the electromagnet longitudinal axis; y coordinate is the position of the electromagnet front face. (a) Position (1, 0) cm. (b) Position (1.5, 0) cm. (c) Position (0, 0.8) cm.

The procedure previously mentioned has been accomplished with different combinations of these variables. The results are shown in next section.

5.2.1 Results of testing using a Susceptometer

In all the experiments it has not been possible to visualize directly if the electromagnet does any effect to SPIONs trajectory. As illustrated in Figure 5.14, the particles have flowed through both channels for all the combinations tested in this work.

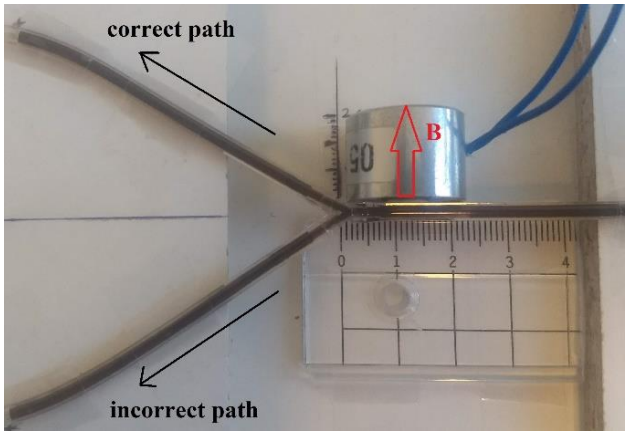

Figure 5.14: Behaviour of the magnetic particles observed in all measuring rounds during testing with susceptometer. The mixture of SPIONs and water flows through both channels, not allowing to visualize any effect on SPIONs. In the present photograph: electromagnet is switched on indefinitely; Q = 1 mL/min; electromagnet in position (1, 0) cm; V_s = 11 V; mixture (1, 2) mL.

First, a mixture of 1 mL of SPIONs plus 2 mL of water has been used. Results of a first round using *V*s = 11 V, being the electromagnet switched on indefinitely and positioned in (1, 0) cm are shown in Figure 5.15.

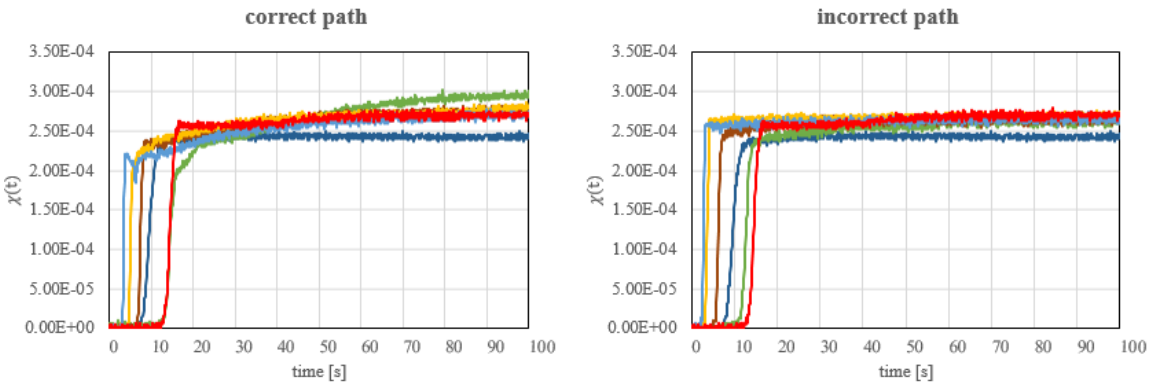

Figure 5.15: Acquired measurements of magnetic susceptibility in both channels after the Y-connector according to different values of flow rate. Mixture (1, 2) mL; Voltage source of the electromagnet V_s = 11 V; electromagnet placed in position (1,0) cm. — baseline (red) — Q = 0.752 (dark blue) — Q = 1 (green) — Q = 2 (brown) — Q = 3 (yellow) — Q = 4 (soft blue). All flow rates in mL/min.

As we can observe, only with a flow rate of 1 mL/min (green) there is an increase in the correct path compared to the baseline, although it is insignificant (the magnetic susceptibility values have the same order and differ less than 5×10^{-5} units). Also, acquired measurements in the incorrect path show an insignificant decrease of magnetic susceptibility compared to the baseline.

Next, keeping a *V*s = 11 V, different positions of the electromagnet have been tested (see Figure 5.16). Although the differences are also not significant, we observe that only for position (0, 1) cm the susceptibilities have increased with the except of that for 0.752 mL/min. We proceed, thus, to use this electromagnet position in next rounds.

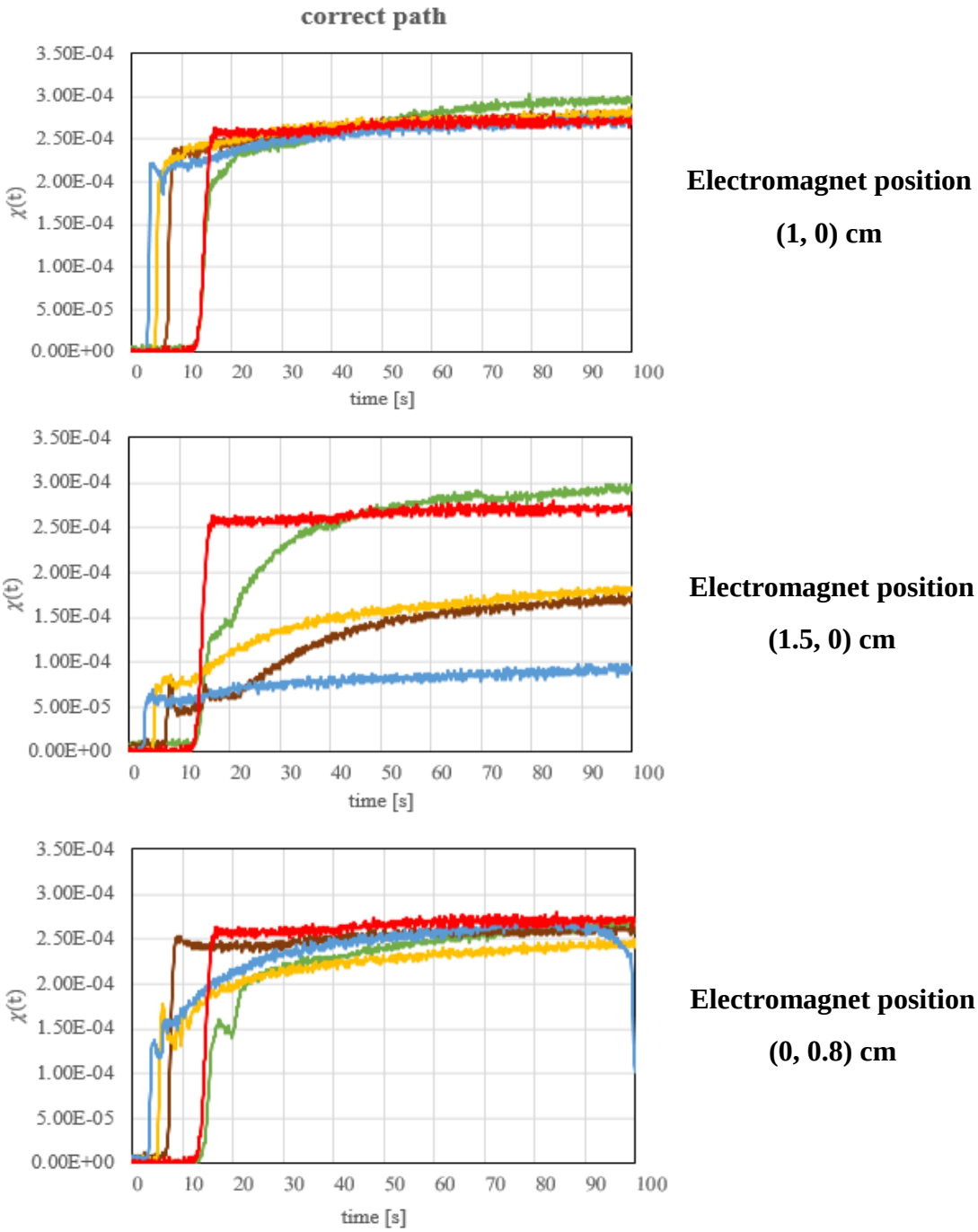

Figure 5.16: Acquired measurements of magnetic susceptibility in the correct channel according to different values of flow rate and position of the electromagnet. Mixture (1, 2) mL; Voltage supply of the electromagnet V_s = 11 V. — baseline (red) — Q = 1 (green) — Q = 2 (brown) — Q = 3 (yellow) — Q = 4 (soft blue). All flow rates in mL/min.

In the following, the efficacy of the switch period of the electromagnet (*T*) has been checked (see Figure 5.17). For that purpose, a flow rate of 1 mL/min has been used because of the better results acquired with such value in previous experiments shown in Figure 5.15.

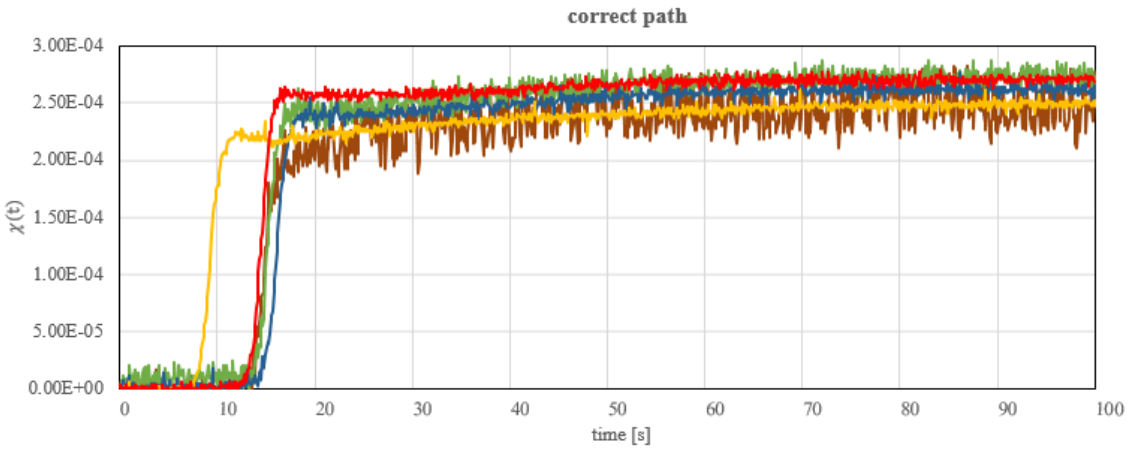

Figure 5.17: Acquired measurements of magnetic susceptibility in the correct channel according to different values of switch period of the electromagnet (*T*). Mixture (1, 2) mL; Voltage supply of the electromagnet V_s = 11 V; electromagnet in position (1, 0) cm; flow rate Q = 1 mL/min. — baseline (red) — *T* = 0.01 s (brown) — *T*= 0.1 s (green) — *T* = 0.5 s (dark blue) — *T* = 2 s (yellow).

The results shown in the figure above indicate there is no difference among the different switch periods. The differences are insignificant, thus, we use the electromagnet switched on indefinitely for next measuring rounds.

Finally, the results acquired according to the different values of the electromagnet voltage supply V_s and flow rates Q are illustrated in Figure 5.18. Although the differences among the magnetic susceptibility of both channels and the baseline are no significant in all cases, we observe that higher voltage sources (V_s = 11 V) and lower flow rates (Q =1 mL/min) approaches more to the initial expected results (an increase of magnetic susceptibility in the correct path and a decrease in the other one). On the other hand, we conclude that lower V_s (6 and 2 V) and higher Q (2, 3 and 4 mL/min) yield bad results. For that situations, the measurement in the incorrect path is higher than the correct path, which is contrary to expected.

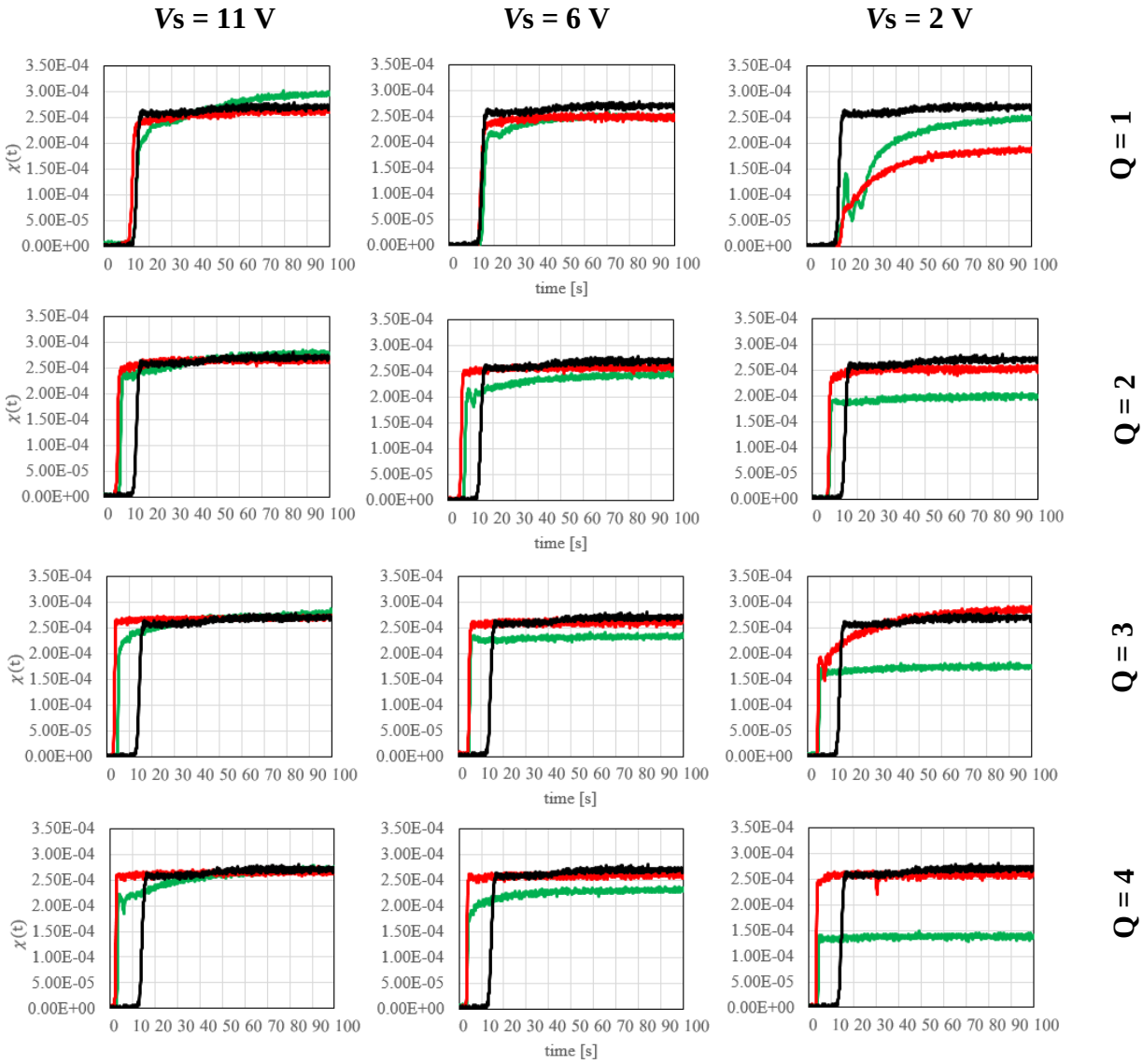

Figure 5.18: Acquired measurements of magnetic susceptibility in both channels after the Y-connector according to different values of voltage source of the electromagnet (V_s) and different values of flow rate (Q). Mixture (1, 2) mL. Electromagnet switched on indefinitely. Electromagnet position: (1, 0) cm. — baseline (black) — correct path (green) — incorrect path (red).

Using a mixture of 4 mL of SPIONs plus 1 mL of water neither we have not obtained good results. Figure 5.19 shows the specific case for a Q = 1 mL/min and V_s = 11 V according to different positions of the electromagnet and taking measurements during 50 seconds. As acquired previously, only the results for an electromagnet position (1, 0) cm shows an expected behaviour of the system, but not significant.

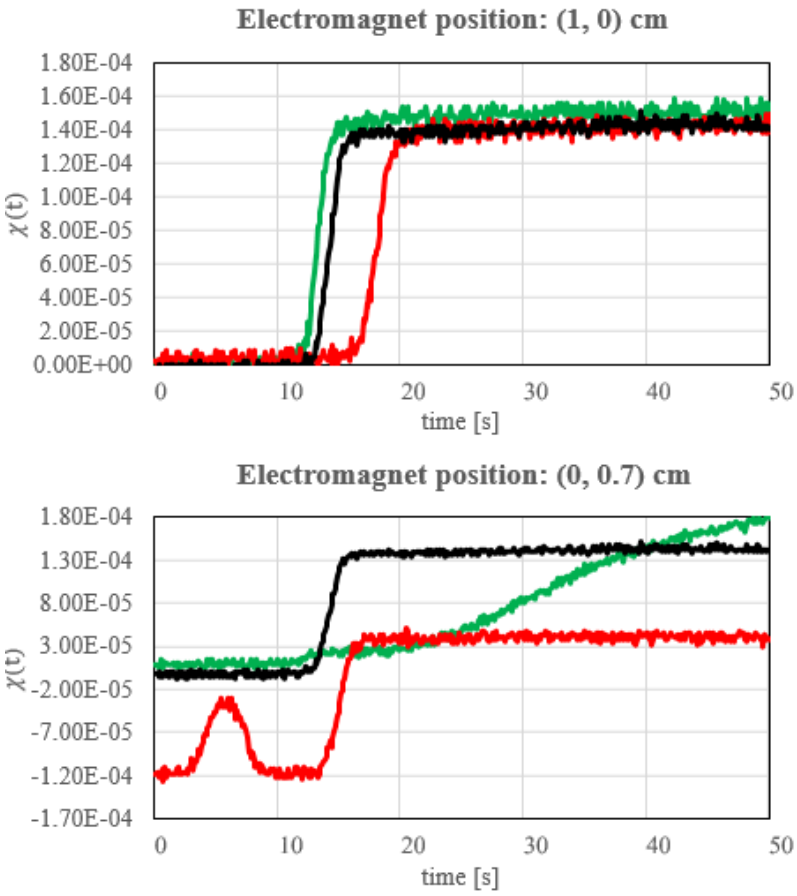

Figure 5.19: Acquired measurements of magnetic susceptibility in both channels after the Y-connector according to different positions of the electromagnet. Mixture (1, 4) mL; V_s = 11 V; flow rate Q = 1 mL/min. Electromagnet switched on indefinitely. — baseline (black) — correct path (green) — incorrect path (red).

Because of these bad results, we have also decided to test with the setup shown in Figure 5.1 from section 5.1 (Testing without Susceptometer), where it is used only one pump and the qualitative results showed that the magnetic field generated by the electromagnet affect the trajectory of the SPIONs, but now adding the susceptometer. Nevertheless, results show again an insignificant difference among measurements of the channels (see Figure 5.20).

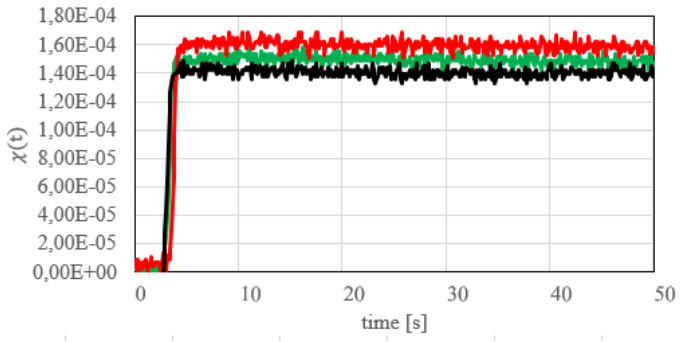

Figure 5.20: Acquired measurements of magnetic susceptibility in both channels after the Y-connector according to different positions of the electromagnet. Mixture (1, 4) mL; V_s = 11 V; flow rate Q = 1 mL/min. Electromagnet switched on indefinitely. — baseline (black) — correct path (green) — incorrect path (red).

The no significant results acquired with the previous combination of variables of the system suggest this electromagnet does not generate enough magnetic force to affect the magnetic particles trajectory; another one with higher force is required. Even then, we could observe how the results approximates more to the expected ones with higher voltage source of the electromagnet V_s (11 V), which means higher magnetic forces. Also, with lower flow rates (Q = 1 mL/min) and positioning the electromagnet in (1, 0) cm.

5.2.2 Problems during Testing

In this section we explain briefly the problem we have had during the realized experiments and its possible relation with the results acquired. In this way, a better measuring procedure can be accomplished in future research work.

The main problem has been the precipitation of the SPIONs. As Figure 5.21 shows, the SPIONs on the left glass are precipitated, which implies they are agglomerated. This is the state at which the nanoparticles are when they have been mixed, for instance, with non-distilled water or other chemical substance. In accomplished testing in this work, oxalic acid has been used in order to remove from the tubes of the testbed any residual particle after each measuring round. If the tubes are not cleaned with proper amount of distilled water after the oxalic acid has flowed through them, it is likely it mixes with SPIONs at next measuring round, causing its precipitation.

Figure 5.21: Glasses with mixtures of SPIONs and water. On the left, a glass with precipitated SPIONs; on the right, a glass with SPIONs in proper state to be used in testing.

This phenomenon has been produced in some of the measurements, causing that the particles agglomerate and stick on the walls of the tubes (see Figure 5.22). When this occurs, the flow of SPIONs can be block, causing failed measurements of magnetic susceptibility.

(a) (b)

Figure 5.22: Precipitation of SPIONs during the testing. (a) SPIONs precipitate and consequently, they are agglomerated. (b) Zoom in of red circle from (a). Precipitated SPIONs tend to stick on the walls of the tubes not allowing the proper flow of the mixture.

Thus, in future research studies of the presented work, it is totally required to ensure that the tubes do not contain residual components like acids or non-distilled water in order to conduct reliable experiments with the magnetic particles.

Chapter 6

Conclusion and Outlook

6.1 Conclusion

As part of this thesis, an optimization of the transmitter setup of a molecular communication testbed based on superparamagnetic iron nanoparticles in duct flow has been developed. For that purpose, the magnetic field generated by an electromagnet has been used in order to try to steer the magnetic particles through a desired path after a Y-connector.

An electromagnet whose size is in proportion to the tubes used in the system has been selected. It has been placed in different positions in the proximity of the splitting, as well as different combinations of other variables of the system have been tested. These variables are the amount of SPIONs and water used in the injected mixture, the flow rate pumped, the voltage supply of the electromagnet and the switch period of the electromagnet. SPIONs with a particle radius of 27.5 nm have been used.

The efficacy of the proposed testbed has been determined measuring magnetic susceptibility changes in both channels after the Y-connector. For this operation, only a susceptometer coil provided by FAU has been used. The ideal procedure would have been to use two devices, so that magnetic susceptibilities in the channels were measured at the same time. In this way, acquired measurements would be more reliable.

For each injection mixture used, a magnetic susceptibility baseline has been registered, which has consisted in measuring the magnetic susceptibility of the system without using the electromagnet. The expected behaviour of the magnetic particles under the influence of the electromagnet was the next: an increase of the magnetic susceptibility in the desired

path after the Y-connector compared to the baseline, where more SPIONs than in the other channel are supposed to flow; on the other hand, a decrease of magnetic susceptibility in the other path.

Experimental results have shown a no expected performance of the system: there is no significant difference among magnetic susceptibilities of both channels and the baseline, neither between both channels. Thus, the magnetic field generated by this electromagnet does not affect the SPIONs trajectory. Even then, acquired results have been closer to the expected ones for a combination of higher voltages sources of the electromagnet (specifically 11 V), which indicates that another electromagnet with higher magnetic force is required. Also, results have been closer for lower flow rates (specifically 1 mL/min) and positioning the electromagnet in such next way: its front face contacting the walls of the tube; its longitudinal axis oriented perpendicularly to the tube and positioned at a distance of 1 cm from the start of the Y-connector.

Furthermore, we have had a big problem during the experiments. The magnetic nanoparticles have been precipitated after they have been used some attempts, which has implied the need to repeat some of the measurements. That phenomenon can be related to the fact that we have used oxalic acid to clean the tubes after each measuring round. This acid may have been mixed together with SPIONs if it has not been used enough distilled water to remove residual particles of that acid and, thus, causing its precipitation. It can also be caused if SPIONs are mixed with non-distilled water. Therefore, in future research work it should be ensured this phenomenon does not occur in order to get more reliable results.

Summarizing, results denote that an electromagnet with higher magnetic field should be selected as well as new experiments should be conducted using new combinations of the variables of the system. Experimentation with larger SPIONs is also suggested. For that purpose, it has been confirmed that FAU can provide SPIONs of approximately 100 nm in the future.

6.2 Outlook

Even though in this work has been used only one electromagnet, in future research work the efficacy of two electromagnets can be tested. One for each channel after the Y-connector, as illustrated in Figure 6.1. SPIONs trajectory can be modified according to a switch period of the electromagnets: electromagnet 1 is switched on some seconds to steer the particles through the susceptometer; after that, electromagnet 1 switches off and electromagnet 2 switches on to guide the particles towards the other channel. In this way, signal propagation in the desired path (channel where the susceptometer is placed) may be clearer.

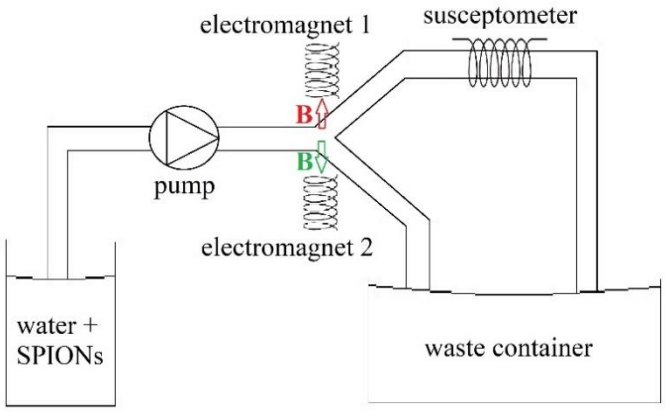

Figure 6.1: Schematic representation of a molecular communication testbed using two electromagnets to steer the magnetic particles through both channels after a Y-connector.

For that purpose, a control circuit as shown in Figure 6.2 would be required.

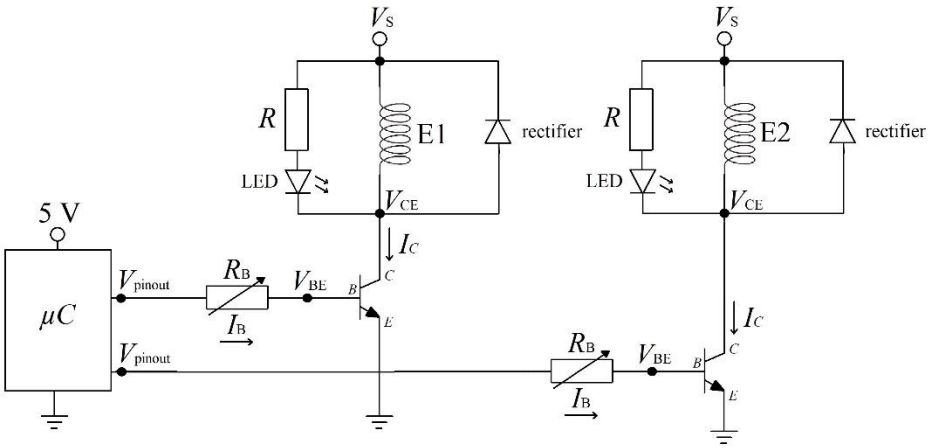

Figure 6.2: Schematic representation of the control circuit to switch automatically two electromagnets.

Because of a new electromagnet with higher magnetic force is required for future experiments and it is likely to allow a different range of voltage supply V_s, the base resistor of the control circuit must be recalculated, according to the procedure followed in section 4.1.2.5 of this document.

In Figure 6.3, we present an example of the programming code to control automatically the switch of both electromagnets.

```
1  #include <xc.h>
2  #include <pic16f690.h>
3
4  //Start of configuration of PIC bits
5  #pragma config FOSC = INTRCIO
6  #pragma config WDTE = OFF
7  #pragma config PWRTE = OFF
8  #pragma config MCLRE = OFF
9  #pragma config CP = OFF
10 #pragma config CPD = OFF
11 #pragma config BOREN = OFF
12 #pragma config IESO = OFF
13 #pragma config FCMEN = OFF
14 //End of configuration of PIC bits
15
16 #define _XTAL_FREQ 4000000
17
18 void main(void)
19 {
20     TRISC = 0b11111100;
21
22     while(1)
23     {
24     //switch on of electromagnet 1
25     PORTCbits.RC0 = 1;
26     __delay_ms(100);
27     //switch off of electromagnet 1
28     PORTCbits.RC0 = 0;
29     __delay_ms(100);
30     //switch on of electromagnet 2
31     PORTCbits.RC1 = 1;
32     __delay_ms(100);
33     //switch off of electromagnet 2
34     PORTCbits.RC1 = 0;
35     __delay_ms(100);
36     }
37 }
```

Figure 6.3: Programming code to switch cyclically two electromagnets using the editor MPLAB X IDE. The microcontroller controls the switch of both electromagnets by pins RC0 and RC1.

One electromagnet receives the signal from the microcontroller by pin RC0 and the other one by pin RC1. Different values of switch period can be tested changing the number of delay commands (lines 26, 29, 32 and 35 in the programming code).

Appendix A

Appendix

The enclosed CD-ROM includes following data:

- Datasheets of the components used in the control circuit to switch the electromagnet
- Simulation file of the control circuit for LTspice®
- Magnetic susceptibility measurements acquired during testing
- Programming codes for the microcontroller:
  - To switch an electromagnet on indefinitely
  - To switch an electromagnet on/off cyclically
  - To switch two electromagnets on/off cyclically
- Recorded videos during testing
- Master thesis: Optimization of the transmitter setup for a molecular communication link based on superparamagnetic iron nanoparticles, by Carlos Martínez Cantón

List of Figures

List of Tables

Bibliography

[1] N. Farsad, H. B. Yilmaz, A. Eckford, C.-B. Chae, and W. Guo, "A comprehensive survey of recent advancements in molecular communication", *IEEE Commun. Surv. Tutorials*, vol. 18, no. 3, pp. 1887–1919, 2016.

[2] H. Unterweger, J. Kirchner, W. Wicket, A. Ahmadzadeh, D. Ahmed, V. Jamali, C. Alexiou, G. Fischer, R. Schober, "Experimental Molecular Communication Testbed Based on Magnetic Nanoparticles in Duct Flow", *2018 IEEE 19th International Workshop on SPAWC*, pp. 1-5, 2018.

[3] Q. A. Pankhurst, J. Connolly, S. Jones, and J. Dobson, "Applications of magnetic nanoparticles in biomedicine", *J. Phys. D: Appl. Phys.*, vol. 36, no. 13, p. R167, 2003.

[4] N. Farsad, W. Guo, and A. W. Eckford, "Tabletop molecular communication: Text messages through chemical signals", *PLoS ONE*, vol. 8, no. 12, p. e82935, Dec. 2013.

[5] A. Ahmadzadeh, V. Jamal, W. Wicke, R. Schober, "Molecular Communication: State-of-the-Art and Challenges", Institute for Digital Communications of Friedrich Alexander Universität Erlangen-Nürnberg, *Kick-off Workshop for EFI Project on Molecular Communication.*

[6] R. S. M. Rikken, R. J. M. Nolte, J. C. Maan, J. C. M. Van Hest, D. A. Wilson, P. C. M. Christianen, "Manipulation of micro- and nanostructure motion with magnetic fields", Institute of Molecules and Materials, Radboud University Nijmegen, The Netherlands, 2013.

[7] NPTEL, *Module 6: Magnetic Ceramics, Paramagnetism*, https://nptel.ac.in/courses/113104005/lecture30a/30_3.htm [Online; accessed on 10/10/2018]

[8] M. Marolt, *Superparamagnetic materials*, http://mafija.fmf.uni-lj.si/seminar/files/2013_2014/superparamagnetic_materials.pdf [Online; accessed on 18/09/2018].

[9] R. V. Ramanujan, *Magnetic Particles for Biomedical Applications*, http://www3.ntu.edu.sg/home/ramanujan/reprints/Bio%20book%20chapter.pdf [Online; accessed on 19/09/2018].

[10] M. Marolt, *Superparamagnetism*, http://eng.libretexts.org/Textbook-Maps/Chemical_Engineering/Supplemental_Modules_(Materials_Science)/Magnetic_Properties/Superparamagnetism [Online; accessed on 18/09/2018].

[11] D. M. Martín, *Development of Nanofiber SPION Supports and Arsenic Speciation Using Synchrotron and Hyphenated Techniques*,

https://ddd.uab.cat/pub/tesis/2013/hdl_10803_129335/dmm1de1.pdf [Online; accessed on 07/10/2018].

[12] Wahajuddin, S. Arora, "Superparamagnetic iron oxide nanoparticles: magnetic nanoplatforms as drug carriers", *NCBI International Journal of Nanomedicine*, vol. 7, pp. 3445-3471, 2012.

[13] E. Carenza, *Engineering Iron Oxide Nanoparticles For Angiogenic Therapies*, https://ddd.uab.cat/pub/tesis/2014/hdl_10803_284861/ec1de1.pdf [Online; acce--sed on 07/10/2018].

[14] *Electromagnet*, http://electromagnetismotelecouax2013.blogspot.com/2013/05/electroiman.html [Online; accessed on 04/07/2018].

[15] L. C Barnsley, D. Carugo, J. Owen, E. Stride, "Halbach arrays consisting of cubic elements optimised for high field gradients in magnetic drug targeting applications", *IOP Scienc*e, *Physics in Medicine & Biology*, vol. 60, no. 21, 2015.

[16] S. S. Shevkoplyas, A. C. Siegel, R. M. Westervelt, M. G. Prentissc, G. M. Whitesides, "The force acting on a superparamagnetic bead due to an applied magnetic field", *NCBI*, *PubMed*, 2007.

[17] Microchip, PIC16F690 Datasheet: *PIC16F690 Pin Diagram*, page 6, https://www.microchip.com/wwwproducts/en/PIC16F690 [Online; accessed on 05/06/2018].